STABILITY, WEAR RESISTANCE, AND MICROSTRUCTURE OF IRON, COBALT AND NICKEL-BASED HARDFACING ALLOYS

SERDAR ATAMERT

DARWIN COLLEGE, CAMBRIDGE

A dissertation submitted for the degree of

Doctor of Philosophy

at the University of Cambridge, November 1988.

To Tülay

PREFACE

The work described in this dissertation was carried out in the Phase Transformations Group at the Department of Materials Science and Metallurgy, University of Cambridge, between October 1985 and November 1988 under the supervision of Dr. H. K. D. H. Bhadeshia. Except where appropriately referenced, the work presented in this dissertation is original and includes nothing which is the outcome of work done in collaboration. This dissertation is less than 60,000 words long and has not been submitted for any degree, diploma or other academic qualification at any other university.

S. ATAMERT
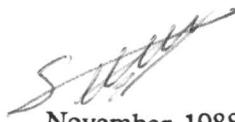
November 1988

ACKNOWLEDGEMENTS

ABSTRACT

This project contributes to the understanding of the effect of alloying elements on the deposit characteristics, microstructure and matrix stability, and wear resistance of iron, cobalt, and nickel-based hardfacing alloys deposited by fusion welding processes. Its primary purpose has been to establish the relationships between microstructure and abrasive wear properties. The effects of arc welding process variables on weld bead dimensions, dilution and microstructure of iron-based hardfacing alloys have been studied using heat flow theory. Theoretical results were compared with experimental data and the agreement was found to be reasonably good.

The microstructure and partitioning ratios of high-chromium and high-carbon hardfacing alloys have been examined experimentally using transmission electron microscopy and microanalytical techniques. The results show that the austenitic matrix is metastable and transforms to ferrite of reduced chromium content, and M_7C_3 carbides. Therefore, the matrix was stabilised by the addition of manganese and nickel. Although this increased the chromium concentration in the matrix, the volume fraction of the primary carbides decreased.

To improve the high-temperature stability, oxidation and corrosion resistance of such hardfacing alloys, the role of Si on their microstructure, phase chemistry and abrasive wear resistance has been examined.

Si is found to partition strongly into the liquid during solidification; Si concentrations of up to 18at% have been found in the matrix, even though the average concentrations used were far less. Si is found to influence significantly the morphology of M_7C_3 carbides, possibly by reducing the orientation dependence of interface energy. This is believed to be beneficial in enhancing the toughness and hence, impact wear resistance of the alloys. A further effect of Si is to reduce the Cr concentration of the austenite in these alloys. This reduction is advantageous because the Cr is used more effectively in the formation of M_7C_3 carbides. The results indicate that high Si alloys have a better abrasion wear resistance, and on the basis of these results new welding electrodes and deposits have already been prepared.

The effect of carbide forming elements (Mo, V, W, Nb, and Ti) on the microstructure and abrasive wear resistance of MMA weld deposits has also been studied. Their partitioning ratios between the matrix and carbide phases and volume fractions of phases have been determined experimentally and the relationship between the microstructure and abrasive wear resistance of these alloys has been analysed.

The microstructure of cobalt-based hardfacing alloys deposited by manual metal arc (MMA) welding, tungsten inert gas (TIG) welding and laser cladding has been investigated to establish the relationship betwen microstructure and abrasive wear properties. For typical deposition conditions, the differences in freezing rates associated with the three processes are found to give rise to large differences in microstructure. The manual metal arc welding process is found to lead to the largest degree of dilution of the hardfacing deposit; the tungsten inert gas and laser clad deposits exhibited much lower levels of mixing with the base plate. For the deposition conditions used in this study, and for the alloys examined, the scale of the microstructures decreases in the

order MMA, TIG and laser cladding, leading to an increase in the deposit hardness in the same order. Other detailed differences in microstructure and phase compositions are discussed and rationalised in terms of process variables.

Abrasive wear test experiments were carried out on these deposits using SiC and Al_2O_3. With alumina, the wear rate is found to be persistently higher with the MMA deposits which have the coarsest microstructure, the weight rate being constant. The laser and TIG deposits which have more refined microstructures and slightly higher carbon concentrations, have both been found to exhibit lower wear rates. The TIG samples initially have been found to be the most resistant to abrasion, even though their microstructure compares with that of the laser samples; this is a consequence of their higher ductility associated with a lower rate of strain hardening. With the much harder silicon carbide abrasive, all samples were found to show similar constant wear rates. The wear data are found to correlate with scanning and transmission electron microscopy observations. The stability of the microstructure at high temperatures has also been examined.

The MMA welding technique was also employed for the deposition of nickel-based alloys. The effect of adding Al and Ti to such alloys on volume fraction and other characteristics of gamma prime precipitates has been studied using a theoretical model capable of accounting for the simultaneous effect of several alloying additions. The experimental results were found to be in agreement with the theoretical approach.

CONTENTS

Chapter Ten:

Comparison of the Microstructures of Stellite Hardfacing Alloys
Deposited by Arc Welding and Laser Cladding

Chapter Eleven:

Comparison of the Abrasive Wear Properties of Stellite Hardfacing Alloys
Deposited by Arc Welding and Laser Cladding

Chapter Twelve:

Microstructural Stability of Co-Based Alloys

Chapter Thirteen:

Nickel-Based Hardfacing Alloys for High Temperature Applications 260

Chapter Fourteen:

Appendix 1: Thermodynamic Program to Calculate Equilibrium Compositions

Appendix 2: Thermodynamic Data

Appendix 3: Coarsening of M_7C_3 Carbides in the Austenite and Ferrite

Appendix 4: Computer Program for Prediction of Weld Bead Dimensions and Dilution

Appendix 5: Welding Terminology

Appendix 6: Computer Program for Ni-Based Alloys

Appendix 7: Scanning Electron Micrographs of High-Si Containing
   Fe-Based Casts

1. AIMS AND SCOPE OF THE PROJECT

Abrasive wear is defined as "wear by the displacement of materials, the displacement being caused by hard particles or protuberances".[1] This definition indicates that abrasion is a part of daily life and is in many cases inevitable. A recent report estimates the losses per annum by friction, wear and corrosion at about 4.5% of the gross national product.[2] The economic importance of wear and the great need for systematic research and a fundamental understanding of wear process has been well recognized.

A knowledge of the microstructure and its influence on wear resistance is of importance for both material selection and alloy development. In other words, the ultimate goal is to predict the changes in microstructure during abrasion, as a function of the wear conditions and initial chemical composition.

Among the wear resistant alloys, hardfacing materials, deposited using one of a wide range of welding processes are used extensively in the form of coatings on a low-cost base material since they improve the desirable properties of a whole component without impairing its bulk properties.

This project aims to lead to an understanding of the microstructure and its influence on abrasive wear resistance, matrix stability, and oxidation and corrosion resistance of iron, cobalt, and nickel-based hardfacing alloys. The flow diagram in Fig. 1.1 illustrates the aims of the project.

Abrasion involves a great number of variables and parameters (e.g. hardness, shape, and size of the abrasives) which make the understanding of the wear phenomena rather difficult. These are examined in Chapter 3, and this knowledge is used for an interpretation of the experimental results in the chapters that follow.

Welding conditions and alloying element additions are the major parameters which control microstructure. The influence of the welding parameters on the deposit characteristics is therefore reviewed (Chapter 2, and 4) and investigated, with the results being presented in Chapters 4 and 5.

It is now becoming widely accepted that in order to further the development of hardfacing alloys one needs a basic understanding of their microstructure. Therefore, the effect of microstructure on abrasive wear, oxidation, corrosion resistance and matrix stability is reviewed in Chapter 6.

On the basis of a detailed literature review in Chapter 6, Chapter 7 aims to understand the microstructural properties of Fe-Cr-C hardfacing alloys, and the effects of a wide range of alloying elements, and subsequently to establish the relationship between abrasive wear resistance and the microstructure. Theoretical calculations are also essential for any alloy design procedure in order to rationalise the effect of alloying elements on the volume fraction and equilibrium compositions of carbide and matrix phases.

1

MICROSTRUCTURAL CONTROL AND
DEVELOPMENT OF HARDFACING ALLOYS

CONTROL OF MICROSTRUCTURE

DEVELOPMENT

PROCESSES

Thermodynamic
Models

MMA TIG PAW LASER CLADDING

to obtain better wear, oxidation,
and corrosion resistance,
to reduce the level of
strategically important and
expensive alloying elements,
(Cr,Co,Mo,V, W.....)

Different heat inputs,
cooling rates, thermal stresses and
contractions, significantly alter the
microstructure.

ALLOYING ELEMENTS

MATRIX   HARD PHASES

Hardness   Stability

Morphology

Volume fraction

Ambient temperature   High temperature
Applications

Effect of microstructure

Wear resistance   Oxidation and Corrosion
Resistance

Fig. 1.1:   Flow diagram illustrating the aims of the project. Where MMA, TIG, and PAW refer
to the manual metal arc, tungsten inert gas, and plasma arc welding processes respectively.

3

2. HARDFACING PROCESSES AND ALLOYS

2.1 Hardfacing

Hardfacing is the application of a hard, wear, oxidation and corrosion resistant material to the surface by welding, spraying, or allied welding processes to decrease wear or destruction of a material under different sorts of service conditions.[1] Fig. 2.1 illustrates the schematic representation of the hardfacing process. This process is more economical than improving the desired properties of the entire component, because hardfacing involves the application of a coating to a low cost base material. The surfaces are generally modified by using welding or allied welding processes excluding the use of extra heat treatments after the deposition.
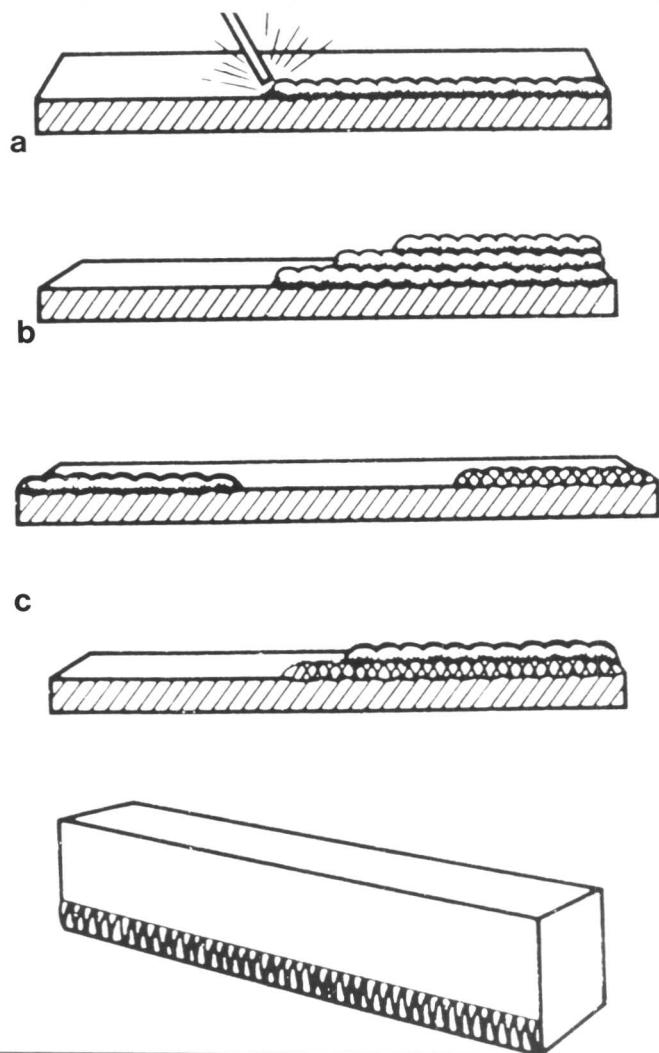
Fig. 2.1: Schematic representation of the hardfacing process. Hardfacing alloys are deposited onto a substrate either as a single (a) or multiple layers (b). In some applications a buffer layer is first deposited and then a hardfacing alloy is added (c) to minimize the difference in thermal contraction between the deposit and base metal.

Since hardfacing is used to improve the service life of the components, the alloys to be deposited should have certain desired properties, as summarised below.

```
1) Hardness
      - macrohardness,
      - microhardness, (the hardness of the individual components in a
        microstructure, e.g. hardness of the carbides)
      - hot hardness, (elevated temperature hardness)
      - creep resistance (for high temperature applications).

2) Abrasion resistance
      - under low-stress abrasion,
      - under high-stress abrasion,
      - under corrosive, and oxidative conditions.

3) Heat resistance
      - oxidation resistance,
      - resistance to thermal fatigue.

4) Corrosion resistance.

5) Tribological properties
      - friction coefficient,
      - surface films,
      - lubricity,
      - plasticity.
```

2.2 Hardfacing Alloys

Conventional surfacing materials are generally classified as steels, or low-alloy ferrous materials, irons or high-alloy ferrous materials, cobalt-based alloys, nickel-based alloys, copper-based alloys, carbides, and chromium boride paste.[2] The classification of weld deposited hardfacing alloys based on their compositions has been proposed by the Hardfacing Working Party of British Steel, and the procedure is summarised in Table 2.1. This table also includes the deposited hardness of each alloy and the most commonly used welding technique. The comparison of properties of hardfacing alloys is represented in Fig. 2.2.

| Classification | | | Typical composition, % (● indicates possible presence) | | | | | | | | | | | | Deposited hardness, HV |
Group		Type	Fe	C	Cr	Mn	Mo	V	W	Co	Ni	B	Nb	Cu	
1 Steels	1	Carbon steels	Balance	0.35											up to 250
	2	Low alloy steels	Balance	0.1–0.5	●	●	●	●	●		●		●		250–650
	3	Martensitic Cr steels	Balance	0.1–1.7	10–15	●	●	●	●		●				350–650
	4	High speed steels	Balance	0.3–1.5	10 max	5	10	3	20	12					600–700
	5	Austenitic stainless steels	Balance	0.07–0.2	17–32	●	●				7–22				(1) 200 (2) 500
	6	Austenitic Mn steels	Balance	0.5–1.0	●	11–16	●	●			●				(1) 200 (2) 600
	7	Austenitic Cr Mn steels	Balance	0.3–0.5	12–15	12–15	●	●			●				(1) 200 (2) 600
2 Irons	1	Austenitic irons	Balance	4	12–20	●	●				●				300–600
	2	Martensitic irons	Balance	1–4	1–10	●	●	●	●		●	●			500–750
	3	High Cr austenitic irons	Balance	3–6	20–40	●	●				●				500–750
	4	High Cr martensitic irons	Balance	2–3	20–30	2 max									500–750
	5	High Cr complex irons	Balance	2–5	20–40	●	●	●	●	●	●	●			600–800
3 Nickel alloys	1	Nickel	8	2		1					85 min				160
	2	Nickel copper	3–6	0.35–0.55		2.5					60–70			25–30	130
	3	Nickel iron	Balance	2		1					45–60				200
	4	Ni Mo Cr W	6	2.5	30 max		17		15	12	Balance		7		250–500
	5	Ni Cr B	●	●	5–25		●	●			Balance	1–5			200–750
	6	Ni Mo Fe	5–20				20–30				Balance				200–300
4 Cobalt alloys	1	Co Cr W low alloy		0.7–1.4	25–32				3–6	Balance					350–400
	2	Co Cr W medium alloy		1.0–1.7	25–32				7–10	Balance					400–500
	3	Co Cr W high alloy		1.7–3.0	25–35				11–20	Balance					500–650
	4	Co Cr W Ni alloys		1.2–2.0	20–25				10–15	Balance	20–25				390–450
5 Copper alloys	1	Brasses	up to 40%Zn balance Cu												130
	2	Silicon bronzes	up to 4%Si balance Cu												80–100
	3	Aluminium bronzes	8–15%Al balance Cu												130–139
	4	Tin bronzes	4–12%Sn balance Cu												40–110
6 Tungsten carbide		Minimum 40% tungsten carbide granules in an iron base matrix or can be in a copper, cobalt, or stainless steel matrix													–1800 (granules)
7 Chromium boride paste	1				80–85						15–20				750–1100

(1) As deposited   (2) Work hardened   *OA Oxyacetylene   MMA Manual metal arc   MIG Metal inert gas   FCAW Flux cored arc   TIG Tungsten inert gas

6

```
LOW ←————————ABRASION RESISTANCE——·—→ HIGH

14%Mn steel        Low alloy      Arc deposited    Oxyacetylene
14%Mn-14%Cr        steel             tube             tube
steel                               carbide          carbide
                                                                  LOW
                                                                   ↑
                                                                   |
                   Martensitic Cr steels                        HEAT AND
                                                                CORROSION
                                                                RESISTANCE
Austenitic                                        Austenitic
stainless                                         and                |
steel              High speed steels             martensitic
                                                  irons

                                                                     |
                                                                     ↓
                   Cobalt and nickel base alloys                  HIGH

HIGH ◄·————————IMPACT RESISTANCE————·—→ LOW
```
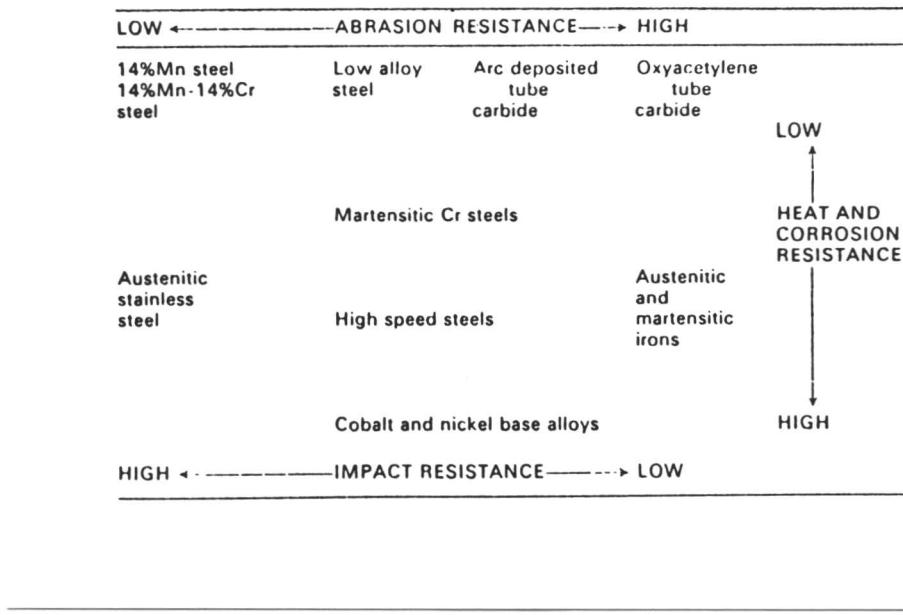
Fig. 2.2: Comparison of properties of hardfacing alloys.[3]

2.2.1 Low-alloy Ferrous Materials

2.2.1.1 Martensitic Steels

These steels are designed to form martensite during the normal air cooling of the weld deposits. These alloys contain up to 0.5C, 3.4Mo, W, Ni and 15Cr (wt%) in order to increase hardenability and strength, and to promote martensite formation. The carbon in these alloys is the major alloying element which influences the mechanical properties. For example, the lower carbon containing alloys are tougher and more crack-resistant than the higher carbon variants. The deposits have high strength with some ductility. However, their abrasion resistance is low although it can be increased with carbon content. The deposits are used for the reinforcement of shafts, rollers and other machined surfaces.

2.2.1.2 High-Speed Steels

These alloys are basically martensitic steels modified with tungsten, molybdenum, and vanadium which form stable carbides so that the alloys remain hard to temperatures as high as 600°C. They are used in the applications where high-speed tool steels are used.

7

2.2.1.3 Austenitic Steels

The austenitic phase in these steels is stabilised by manganese additions. The steels can be categorised into two groups; the low-chromium, and high-chromium alloys. Low-chromium alloys (up to 4.0Cr, 12-15Mn, Ni, Mo wt%) are tougher due to the absence of hard chromium carbides and are used under high impact service conditions. High-chromium austenitic steels (12-17Cr, 15Mn wt%) are used for rebuilding manganese steel and carbon steel parts which experience metal-to-metal pounding, as well as for joining manganese steels. Although these alloys are relatively soft in as-deposited condition, they rapidly work-harden as a consequence of surface deformation.

2.2.2 Ferrous Materials

High alloy irons contain large amounts of chromium and/or molybdenum additions which form the carbides that impart abrasion resistance. The matrix may be austenitic, martensitic, pearlitic, ferritic or some combination of these phases. The high carbon (2-6, wt%) and high chromium (up to 40 wt%) concentrations provide a large volume fraction of hard M_7C_3 carbides which enhance wear resistance and the chromium also promotes the formation of oxide layers (e.g. Cr_2O_3) so that these alloys are occasionally used in situations requiring oxidation resistance (e.g. rolling mill guides[4]). Some iron-based hardfacing alloys contain up to 5.0Ni and 8.0Mn (wt%) to stabilise the austenitic phase and to reduce the tendency of cracking during cooling.[1]

Low-alloy hardfacing irons contain up to 15Cr (wt%) and some molybdenum and nickel in the austenitic matrix. They show excellent low-stress abrasion resistance since thay have a smaller volume fraction of brittle carbides.

Martensitic irons which are cheaper show good high-stress abrasion resistance primarily because of the high hardness of the martensitic matrix.

2.2.3 Nickel-Based Hardfacing Alloys

These alloys are generally deposited to improve the wear resistance during service at high temperatures. Carbon containing Ni-Cr-Mo-W-C alloys are also gaining popularity as a replacement for the more expensive cobalt-based alloys. The carbon forms M_7C_3 and/or M_6C type carbides which precipitate in a fcc matrix phase which is solution strengthened. Molybdenum and tungsten additions improve the hot hardness and high temperature strength.

Boron containing Ni-based alloys are also available in which the presence of very hard chromium borides provide exceptional abrasion resistance.

Laves phase containing nickel-based alloys (Ni-32Mo-15Cr-3Si wt%) have also been succesfully used in situations where metal-to-metal wear takes place. They unfortunately have poor impact resistance due to the large volume fraction of hard intermetallic precipitates.

8

2.2.4 Cobalt-Based Hardfacing Alloys

Cobalt-based hardfacing alloys have been used widely for over 50 years because of their good wear, oxidation, and corrosion resistance combined with high hot hardness at temperatures sometimes approaching 980°C.[5] The most commonly used Co-based hardfacing alloys are of the "Stellite" variety, with a nominal composition of Co-28Cr-4.0W-1.1C (wt%). First Stellite alloys were developed in 1900 by Elwood Haynes and since then intense efforts have been made in order to modify these alloys.

2.2.5 Copper-Based Alloys

These alloys are used primarily to improve corrosion, cavitation erosion, and metal-to-metal wear resistance although they have poor abrasion resistance.

2.2.6 Tungsten Carbide Composites

Tungsten carbide containing alloys are especially good for heavy abrasive wear conditions. In welding processes, filler material is provided in the form of mild steel tubes containing a mixture of WC and W_2C carbides. The resulting deposits contain undissolved carbides which provide excellent abrasive wear resistance.

2.3 Applications of Hardfacing Alloys

Tha applications vary widely, ranging from the most severe, such as rock crushing, to those which minimize metal-to-metal wear such as control valves where a few thousandths of an inch of wear is intolerable.

Typical applications of hardfacing alloys having a high volume fraction of primary carbides are illustrated in Fig. 2.3a,b. The shovel teeth are made of low-alloy cast steel, and on rare occasions of Hadfield steel. The service life of new teeth and repaired teeth can be increased significantly by hardfacing. The alloys also provide very good abrasion resistance in applications where the leading edges are subject to heavy wear.

Cobalt and nickel-based hardfacing alloys are used extensively at elevated temperatures and in corrosive environments. Hot shear-blades (Fig. 2.3c) and valve seats (Fig. 2.3d) are hardfaced by Stellite type cobalt-based and Hastelloy type nickel-chromium alloys which provide high strength at temperatures above 800°C.
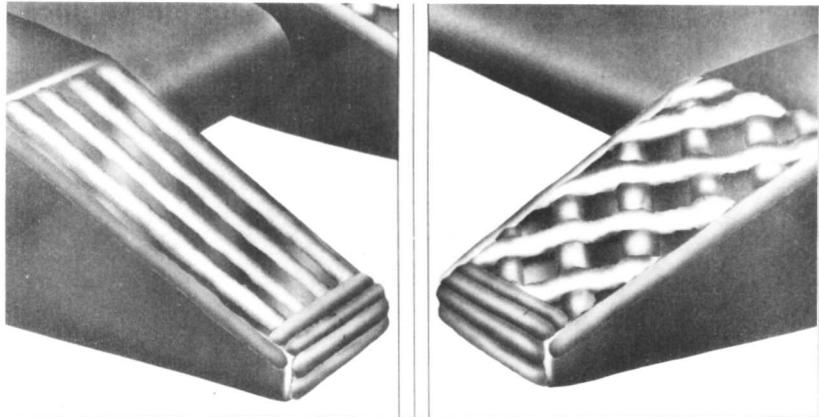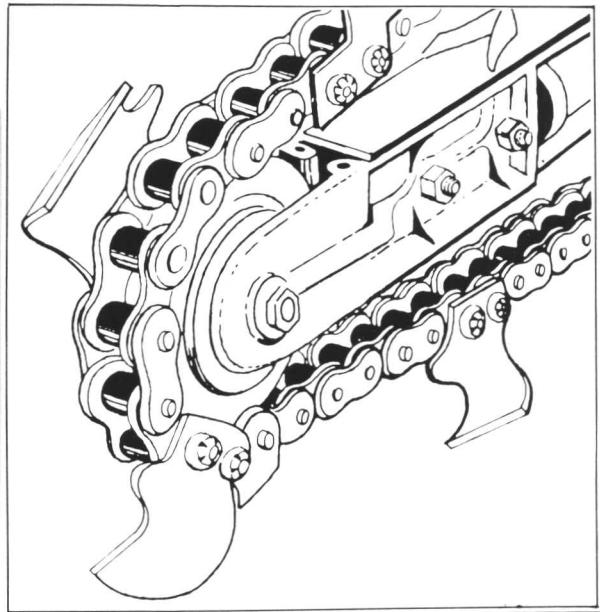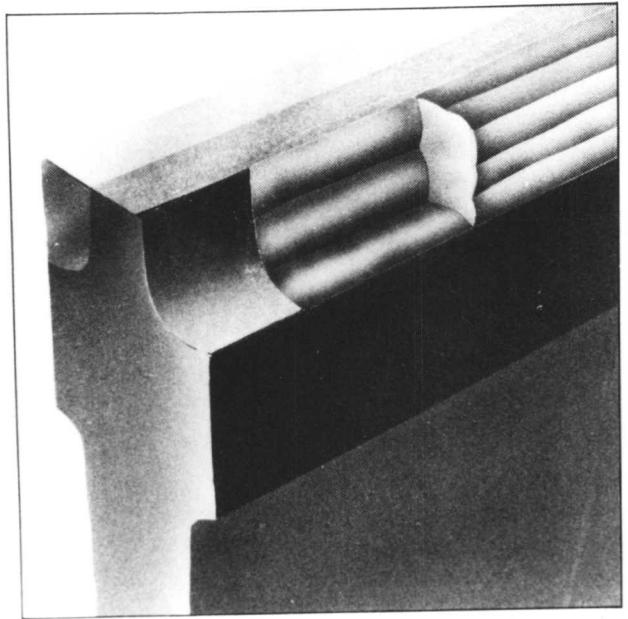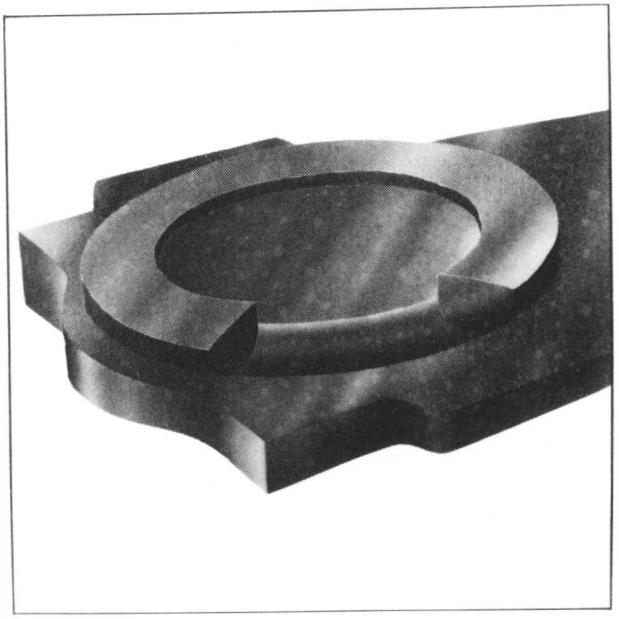
Fig. 2.3: Typical applications of hardfacing alloys. Iron-based hardfacing alloys with a high volume fraction of carbides are used extensively under very severe service conditions, a) shovel teeth; b) trencher teeth. Cobalt and nickel-based hardfacing alloys are preferable for high temperature applications where high temperature strength is very important, c) hot-shear blades; d) valve seats.[6]

2.4 Hardfacing Alloy Selection

Alloy selection is generally considered in terms of a compromise between wear and cost. Other important parameters which must be taken into account are the base metal, deposition process, corrosion and oxidation capacity. In general the following steps should be considered when choosing an alloy:[1]

1) the service conditions,

2) selection of the hardfacing alloy,

3) compatibility of the hardfacing alloy with the base metal,

4) hardfacing process,

5) the level of dilution and the overall cost.

2.5 Property and Quality Requirements

The choice of a hardfacing material usually depends on the deposition process, the component geometry, and the deposition rate, rather than microstructural advantage.

The alloys can be deposited by gas and arc welding, manual metal arc welding, flux-cored arc welding, submerged-arc welding process and spraying techniques. Research comparing the methods is rather limited.

Dilution is a most important parameter which influences the properties of the deposit and substrate. It is defined as the percentage of the base metal that mixes with the hardfacing deposit.[1] A dilution of 30% thus means that the deposit contains 30% base metal and 70% of the original hardfacing alloy. Wear resistance and other desirable properties dependent on dilution, service performance decreasing with dilution. Welding processes and techniques have to be selected so as to control dilution to less than 20%. Hardfacing alloys can be deposited in several layers to minimise the effect of dilution.

2.6 Metallurgical Characteristics of the Base Metal

The choice of a base metal depends upon its composition, melting temperature range, contraction and thermal expansivity.

Steels are generally selected as a most suitable base metal for hardfacing. Medium carbon steels (up to 0.4C wt%) can be hardfaced by most welding processes. For higher carbon steels, austenitic stainless steels, nickel-based alloys, martensitic steels and die steels greater attention to preheat, interpass temperature and stress-relief heat treatment is required.

The difference in thermal expansion coefficient between the deposit and base metal effects the solidification strain. Workpieces have to be uniformly heated to obtain a deposit without cracks. Contraction and thermal expansion differences between the base metal and hardfacing alloy cause the formation of shear failures in some circumstances. Buffer layers are deposited between the base metal and hardfacing material to accommodate better any differences in expansion characteristics.

11

2.7 Surfacing Techniques

2.7.1 Surfacing by Arc Welding

There are many arc welding processes for hardfacing.[4] Some of them are suitable for small, precise overlays, whereas others offer high deposition rates for surfacing larger areas. Large components often have to be surfaced (e.g. blast furnace bell, pressure vessels) using a low heat input to avoid distortion. The manual metal arc welding and tungsten inert gas welding techniques will be summarised here since these processes are extensively used and also are examined in this thesis.

2.7.1.1 Manual Metal Arc Welding (MMA)

The manual metal arc welding is an arc welding process in which coalescence of metals is produced by heat from an electric arc that is maintained between the tip of a covered electrode and the surface of the base material in the deposit being welded (Fig. 2.4). The arc power may be from a direct or alternating current. The arc and the weld pool are shielded by the slag formed from the electrode coating and by the gases evolved from the decomposition of coating materials in the first layer. The thickness of a deposit varies from 3mm upward and dilution may be 10-30% depending on the welding conditions.[4]

A wide range of alloys can be deposited including low and high alloy steels, stainless steels, nickel-based and cobalt-based alloys.

The detailed effects of heat input, travel speed, electrode diameter etc. on deposit properties will be discussed in Chapters 4 and 5.
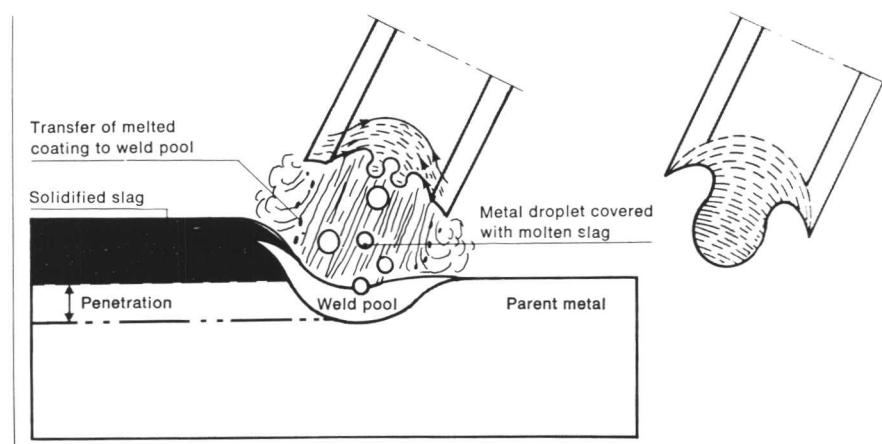
Fig. 2.4:   The manual metal arc welding process.[4]

2.7.1.2 Gas Tungsten Arc Welding (GTAW) Process

In this process, an arc between a nonconsumable tungsten electrode and the workpiece provides the heat source for melting a consumable filler wire (Fig 2.5).

High quality, reproducible deposits can be made using automatic GTAW by controlling filler-metal feed rates, torch oscillation, and travel speed. Many different metals can be surfaced and the base metal thickness changes from 6mm to 100mm, but much thicker sections can be surfaced by this process. Surfacing materials can be high alloy steels, stainless steels, nickel and nickel-based alloys, copper and copper-based alloys, cobalt and cobalt-based alloys. The gas tungsten arc process is basically a low deposition rate process that produces a high quality deposit with a minimum of dilution and a low degree of distortion.
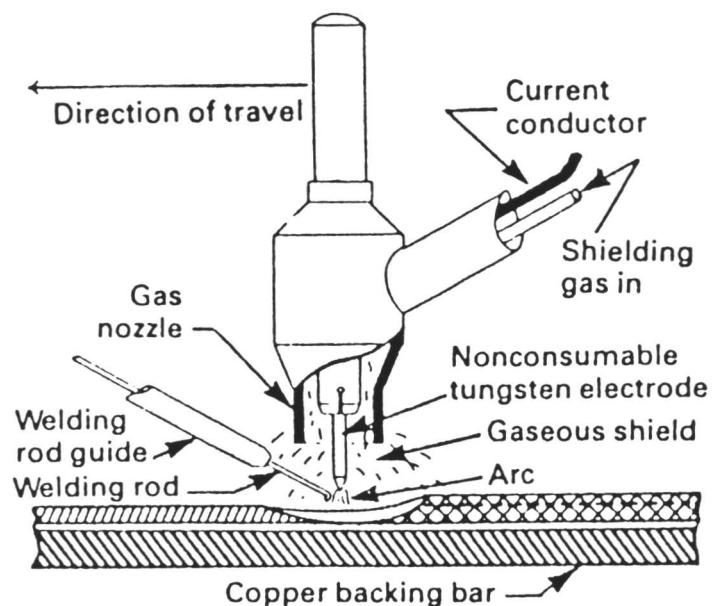
Fig. 2.5: The gas tungsten arc welding process.

2.7.2 Hardening of Metal Surfaces by Laser Processing

Laser processing techniques, used to improve the wear resistance of metals, became feasible with the advent of high power continuous wave carbon dioxide lasers (CW-CO_2). The technology has not yet been fully exploited by researchers in the area of tribology even though many tribologically related surface failures can be minimized by laser surface modification techniques such as laser surface alloying, laser cladding.[7]

From a tribological standpoint, these surface modification techniques can be useful in applications where surfaces are subjected to severe environmental conditions and lubricating films between contacting surfaces cannot be generated because of limited or no lubrication or because of the kinematics or the geometry of the mating parts.

Examples of applications where surface modifications can play a dominant role include stationary and seal components of gas turbines, components in nuclear reactors and internal combustion engines, components in space and vacuum environments and barrels of guns and cannons.

Process techniques include laser alloying, laser cladding, laser melt/particle injection, transformation hardening and laser glazing.[7]

The main advantage of using laser heating is that the surface can be heated with minimal heat transport into the bulk of the component while it reaches the required temperature, thus permitting conduction quenching which hardens the surface to some desired depth. The other general advantages are:

-treatment can be localized to the required area;

-heat input is low, giving minimum thermal distortion of the component;

-almost no machining is required after treatment;

-this process can be applied to complex shapes;

-the laser beam can be directed by mirrors to treat inaccessible areas of components;

-most treatments are rapid.

The methods of laser surface treatment of materials have been classified into three types, those involving heating, melting and thermal shocking can be seen in Fig 2.6. They can also be divided into those relying on a metallurgical change in the surface of the bulk material (Fig. 2.6).

14
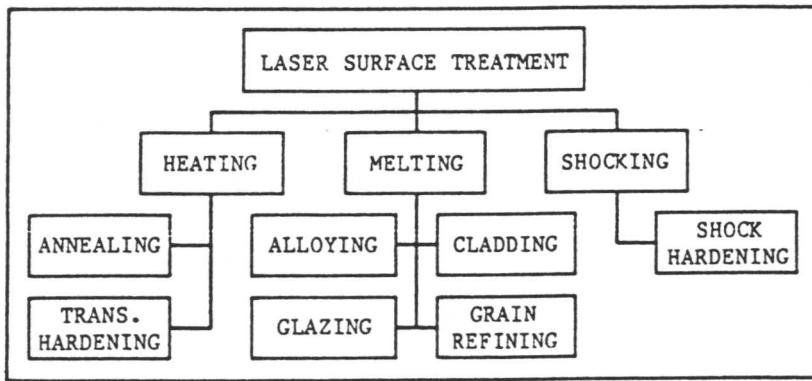
Fig. 2.6: Methods of laser surface treatment of materials.[7]

2.7.2.1 Laser Cladding

Laser cladding differs from surface alloying in that only enough substrate material is melted to ensure good bonding of the applied coating. It differs little in principle from traditional forms of weld cladding, but its advantages are evident when thin claddings are desired or when access to the clad surface can be achieved more readily by a laser beam than with an electrode or torch. The potential for producing novel materials by this process are numerous because of the almost infinite material combinations which can be used for coating.

Laser beams have the potential of applying cladding alloys with high melting points on low-melting workpieces. The cladding alloys are usually cobalt, nickel or iron-based and are used for applications involving metal-to metal wear, impact, erosion, corrosion and abrasion. A single cladding alloy cannot satisfy all the applications mentioned above; consequently, selection of cladding alloys is based on factors such as service conditions, base materials, cladding processes and cost. Laser cladding by powder fusion has recently been used by Rolls Royce for hardfacing turbine blades of aircraft engine.

Laser cladding has many advantages over alternative methods such as plasma spraying and arc welding. These include a reduction in dilution, a reduction in waste due to thermal distortion, a reduction in deposit porosity and machining costs because the material can be placed more accurately. The process also produces good metallurgical bonds. The moderately high quenching

15

rates inherent in this process offer the possibilities of producing novel microstructures.

There are two methods which are extensively used for cladding (Fig. 2.7). In the preplaced powder method a powder for cladding is amalgamated with binders to form a paste which is spread over the substrate. It has been demonstrated that surface layers having complex microstructures with good tribological performance and strong bonds to the base material can be obtained using this process. It is difficult to clad substrates of irregular shape by preplacing a powder layer on the substrate because of the difficulty of maintaining a uniform layer at the desired sight. Weerasinghe and Steen[8] studied another powder delivery method, where the powdered material is directly delivered into the laser substrate interaction region, a process which has more flexibility and versatility during production. They studied the effect of the process parameters on the quality of the cladding layer and pointed out that the powder continuously impinging on the melt pool appeared to give enhanced energy absorption.

a
b
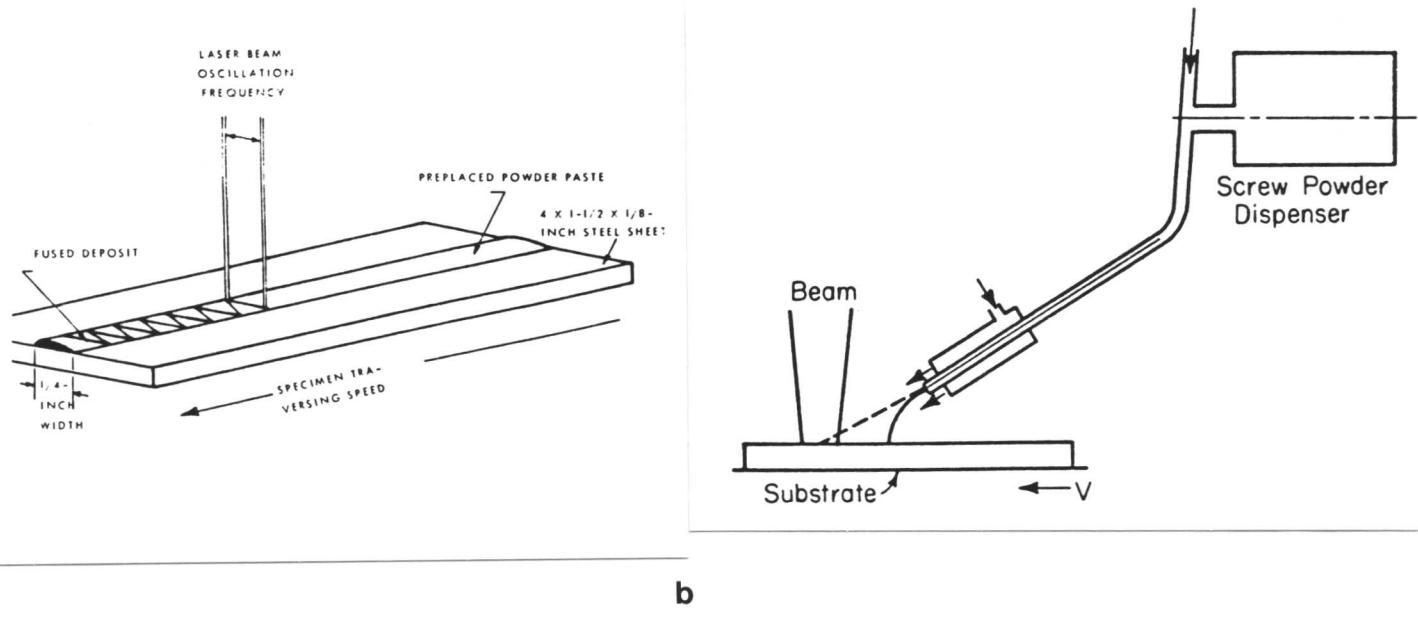
Fig. 2.7: Schematic representations of laser cladding processes, a) preplaced powder; b) powder injection method.

A laser cladding process by powder fusion is mainly a heat transfer controlled process. The laser beam heats and melts the powder and the heat transfers to the substrate until the molten powder layer wets the substrate and bonds with it.

Laser cladding process at best requires both the clad layer and the substrate to maintain their composition with minimum dilution except the small boundary layer.

In order to obtain a high solidification rate and thus a fine microstructure, and a low degree of dilution the specific energy input for the process should be as low as possible. High specific energy input leads to grain coarsening, dilution of clad layer and distortion. Low specific energy input will also make this process more economical and competitive to other alternative methods.

2.7.3 Comparison of Surfacing Processes and Hardfacing Process Selection

In addition to the surfacing processes discussed in this section, oxyacetylene surfacing, submerged arc welding, gas-metal-arc welding, thermal spraying, and plasma-arc-powder surfacing techniques are used extensively. For many applications the appropriate welding method has been established after many years experience. However, any welding process is easily adaptable to more than one mode of application, since the deposit properties depend on the welding parameters (e.g. the arc voltage, current, arc speed). Identical microstructures can be achieved with two different surfacing methods by choosing the correct welding variables.

As a general guideline, hardfacing property and quality requirements, physical characteristics of the workpiece, metallurgical properties of the base metal, form and composition of the alloy, and the required life of the alloy under the service conditions should be considered when choosing the process.

2.8 Summary

Hardfacing materials are used extensively for applications where the surfaces are subjected to wear, oxidation, and corrosion. This is highly economical since it improves the desired properties of the surface of a component without influencing its bulk properties. A wide range of hardfacing alloys are deposited including iron-based, cobalt-based and nickel-based alloys. Hardfacing alloy selection needs careful assessment of the service conditions and a knowledge of material properties specific for the application.

Control of wear starts with the choice of the correct deposition technique and its variables. The alloys can be deposited by a wide range of techniques such as arc welding, plasma spraying and laser cladding. It is not feasible to rank the processes in any order of excellence; such a ranking would in any case be unsuccessful since the choice of process is highly application dependent and any welding process is adaptable to more than one mode of application.

2.9 REFERENCES

1) Metals Handbook, 9th edn, 1983, 771, ASM, USA.
2) R. A. PACEY: Chromium Review, 1985, **5**, 32.
3) E. N. GREGORY: Metal Construction, 1980, December, 685.
4) Welding Handbook, 7th edn, **79**, 1981, Am. Welding Soc. FL.
5) Repair Welding Handbooh, ESAB.
6) P. OAKLEY: in Proc. Conf. 'Surface Engineering 1st International Conference', Paper 62.
7) D. GNANAMATU: in Proc. Conf. 'Applications of Lasers in Materials Processing', 1979, 177.
8) V. WEERASINGHE, and W. STEEN: in Proc. Conf. 'Applications of Lasers in Materials Processing, 1979.

3. TRIBOLOGY AND WEAR

3.1 Introduction

The development of new hardfacing alloys is potentially of large economic importance. In the UK alone, some five hundred million pounds might be saved per annum if significant improvements in wear resistance can be made.

In the past hardfacing alloys have been developed principally using semi-empirical techniques and there is an increasing need for a more systematic approach, not least because of the high cost of the large concentrations of alloying elements used. The best way to develop new hardfacing alloys in the future is expected via a better knowledge of the wear-microstructure relationship.

3.2 Tribology

Tribology is the new name for any problem concerned with the carrying of load across interfaces in relative motion.[1] Thus, although the word is new, the subject concerns itself with such well known topics of friction, wear and lubrication. The name "Tribology" is derived from the Greek words tribos meaning "rubbing" so that a literal translation would be the science of rubbing. This interpretation is a little too narrow, so that the word is actually defined as: "the science and technology of interacting surfaces in relative motion and of related subjects and practices". Tribology is still one of the least developed scientific fields both because of the limited attention it has received and because of its complex and interdisciplinary character.

3.2.1 Economic Aspects of Tribology

The lubrication report[1] estimated in 1966 that, within an error of 25%, an amount exceeding five hundred million pounds per annum could be saved in the civilian sector of the UK economy by improvements in education and research in tribology. Tribology plays a major role in material and energy conservation. As wear is a principal cause of material wastage, any reduction of wear can effect considerable savings. The wear problem may be solved by a better understanding of the mechanisms involved and the parameters which affect wear.

3.3 Wear

Wear is one of the three most commonly encountered industrial problems leading to the replacement of components and assemblies in engineering; the others are fatigue and corrosion. Wear is rarely catastrophic, but it reduces operating efficiency by increasing the power losses, oil consumption, and the rate of component replacement. There is some debate concerning the classification of wear modes. However, most tribologists agree on the following classification of wear.[2]

- <u>Adhesive Wear</u>
- Oxidative wear
- Metallic wear
- Galling

- <u>Abrasive Wear</u>
- Low-stress scratching abrasion
- High-stress grinding abrasion
- Gouging abrasion

- <u>Erosion</u>
- Particle impingement
- Cavitation

- <u>Fretting</u>

3.3.1 Adhesive Wear

Adhesive wear generally describes wear due to the sliding action between two metallic components where no abrasives are intended to be present. When the applied load is sufficiently low, an oxide film is usually generated as a result of frictional heating accompanied by sliding. The oxide film prevents the formation of a metallic bond between the sliding surfaces, resulting in low wear rates. This form of wear is called oxidative or mild. If the applied load is high, formation of a metallic bond occurs between the surfaces of mating materials. The resulting wear rates are extremly high. This form of wear is called severe or metallic wear. Another form of wear, called galling, is a special form of severe adhesive wear. Galling occurs if the wear debris is larger than the clearance and if seizure of the moving component results. Frequently, only small amounts of sliding result in galling and subsequent failure of a component. In situations where lubrication is not possible, hardfacing is recommended to minimize adhesive wear, such as in automotive exhaust valves that experience extreme temperatures at which many lubricants are not stable. Generally most moving components should be designed to resist mild wear.

3.3.2 Abrasive Wear

Low-stress scratching abrasion occurs from a cutting action by sliding abrasives stressed below their crushing strength. In this kind of abrasive wear, worn surfaces contain scratches and the amount of subsurface deformation is minimal. High-stress grinding abrasion occurs under conditions where the stress is high enough to crush the abrasive. In this type of wear, stresses are high enough to cause gross plastic deformation of the ductile constituents. Gouging abrasion describes high stress abrasion where gouges or deep grooves are created on the wearing surfaces. Abrasive wear mechanisms and the effect of the abrasives will be discussed later on in detail.

3.3.3 Erosion

Impingement erosion occurs under the cutting action of a fluid-borne moving particle. The contact stress arises from the kinetic energy of a particle flowing in an air or liquid stream as it encounters a surface. Impingement erosion varies with the angle of impingement. Cavitation involves the collapse of air bubbles caused by the turbulence. When these bubbles collapse on the material surface, wear occurs by the resultant shock waves. This type of wear is called cavitation erosion.

3.3.4 Fretting

This wear phenomenon occurs between two surfaces having oscillatory relative motion of small amplitude. It is a combination of abrasive and oxidative wear.

3.4 Abrasion

Abrasive wear is the displacement of materials caused by the presence of hard particles, between or embedded in one or both of the two surfaces in relative motion, or by the presence of hard protuberances on one or both of the relatively moving surfaces.[3] Abrasive wear can be classified as two-body or three-body abrasion (Fig. 3.1). The former describes the wear caused by sliding on a material so that abrasive particles move freely (Fig. 3.1a). The latter describes the wear caused by abrasive particles trapped between two moving surfaces. It is well recognized that the weight loss is about one to two orders of magnitude smaller in three-body abrasion than in two-body abrasion. This is because in three-body abrasion a small proportion of the abrasives cause wear, due to variations in the angles of attack.
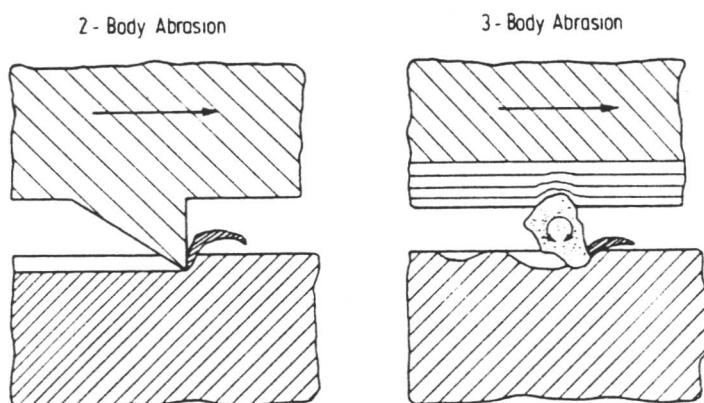

Fig. 3.1:   Abrasive wear modes; a) two-body; b) three-body abrasion.[10]

21

3.4.1 Mechanisms of Material Removal

There are three main mechanisms of material removal during abrasive wear: ploughing, cutting, and spalling (Fig. 3.2). Ploughing occurs as a result of considerable plastic deformation within the wear path and causes material to be heaped up on either side of the the wear groove (Fig. 3.2a). Since this process involves fairly ductile plastic deformation at the surface, the abraded material is not detached so that there is virtually no volume loss during a single-pass of an abrasive particle. Volume loss does of course occur as a consequence of the action of many abrasive particles since the material can only tolerate a finite amount of deformation before fracture.

In microcutting, the material displaced from the groove is removed by fracture resulting in the formation of machining chips, shavings, fragments, etc. (Fig. 3.2b), and there is an obvious material loss corresponding to the volume of wear grooves. Although ploughing and cutting may generally apply to ductile surfaces, this is not always the case.[4] It has been demonstrated that the ratio of microploughing to microcutting, depends upon the attack angle, α^* of the abrasive.[5]1 A transition from microploughing to micocutting occurs when the attack angle exceeds the critical attack angle α_c. It has been shown that the α_c for microchip formation varies widely, since it depends on the friction between the leading face of the abrasive particle and the worn material.[6] The effect of the attack angle on the ratio of cutting to ploughing is illustrated in Fig. 3.3. This figure clearly demonstrates that an increase in the attack angle leads to a high weight loss, as confirmed by experimental results.[7] The wear mechanism changes from pure microploughing to microcutting by increasing the hardness of worn material. This is also consistent with the fact that the critical angle decreases as the hardness increases (e.g. in steels).[8] This has been recently shown in-situ observations in a scanning electron microscope using a single-point scratch test in steels. The results showed that the abrasive wear mechanism changes from ploughing to a wedge formation mode, and then to a cutting mode as the degree of penetration increases. Fig. 3.4 illustrates the wear mode diagram as a function of the hardness of a material, the attack angle, and the degree of penetration. This diagram demonstrates that the value of D_p^* (which corresponds to the transition from ploughing to wedge mode) is independent of the hardness. However, D_p^{**} (which corresponds to the transition from wedge forming mode to cutting mode) decreases with increasing hardness, indicating that the probability of cutting mode is higher than the wedge forming as the hardness increases.

It has been concluded that if the local surface strain exceeds a critical value, then wear occurs by relatively brittle fracture (spalling). With brittle materials, the critical strain can be rather low, and spalling is a common mechanism of wear in materials which lack toughness; it can sometimes be observed locally in the harder phase (e.g., carbides, intermetallic compounds) of wear resistant alloys.

---

[1] The attack angle describes the angle between the leading face of the abrasive particle and ungrooved surface (See Fig. 3.3).
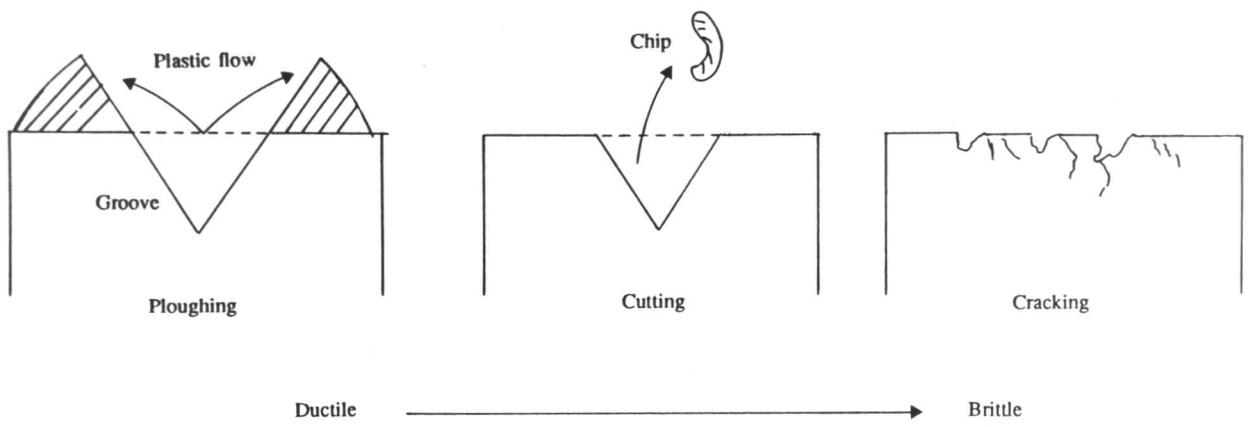
Fig. 3.2: Schematic illustration of the mechanisms of material removal during abrasion.
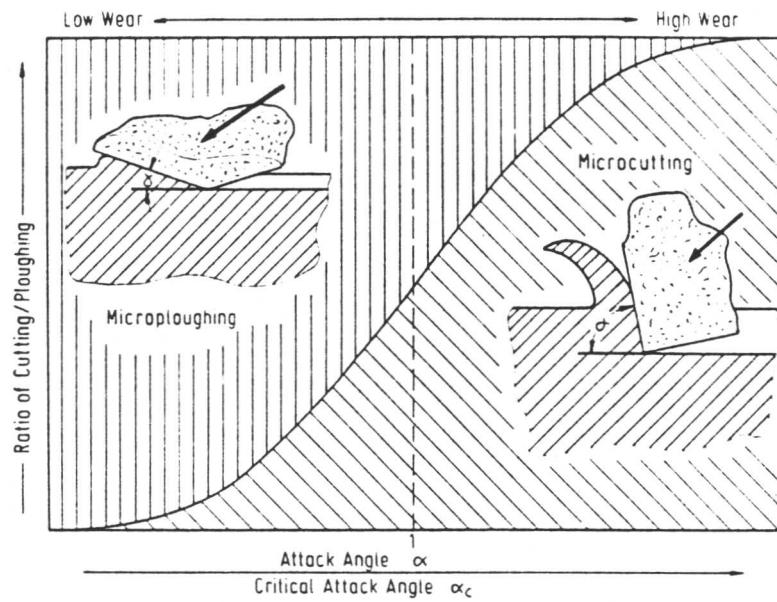
Fig. 3.3: Ratio of microcutting to microploughing as a function of the ratio of the attack angle to the critical attack angle.[5]
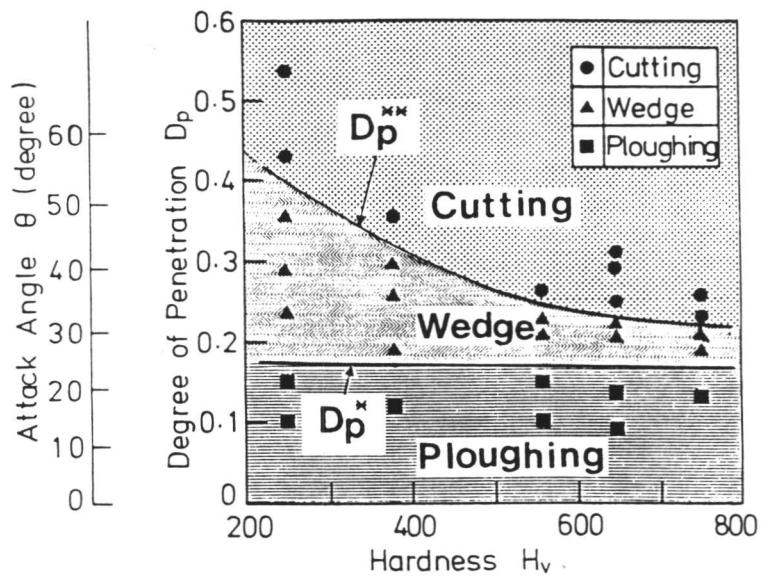
Fig. 3.4: Wear mode diagram as a function of attack angle, degree of penetration, and hardness in steels.[8]

3.5 Quantitative Expression for Abrasive Wear

There have been a number of models for the quantitative representation for abrasive wear.[9] However, a simplified model[10] and its application will be discussed in this section. In this model the asperities carrying a load, ΔL, penetrate the surface to an extent given by

$$\Delta L = p \, \Delta A = p \, \pi \, r^2 \qquad \qquad .....(1)$$

where p is the hardness of the surface. When the abrasive moves through a distance dl, (see Fig. 3.5) it will sweep out a volume ΔV, which is given by

$$dV = rxdl = r^2 \, \tan\theta \quad dl = (\Delta l \, \tan\theta \, dl) / (\pi \, p) \qquad \qquad .....(2)$$

and consequently

$$dV/dl = (\Delta L \, \tan \theta \,) /\pi \, p \qquad \qquad .....(3)$$

where x is the penetration depth, and the rx is the projected area of the penetrating abrasive. This equation is re-written to represent the contributions of all the abrasives as follows;

$$dV/dl = L \, \tan\theta \,/\pi \, p \qquad \qquad .....(4)$$

where $\tan\theta$ is a weighted average value of the $\tan\theta$ values of all the individual cones.

This equation has been applied to pure metals in two-body,[11] and three-body[12] abrasion representing variations of abrasive wear resistance (dl/dV) as a function of hardness (Figs. 3.6, 3.7). The correlation is found to be good for pure metals. but not for multiphase microstructures, as will be discussed in Chapter 6.
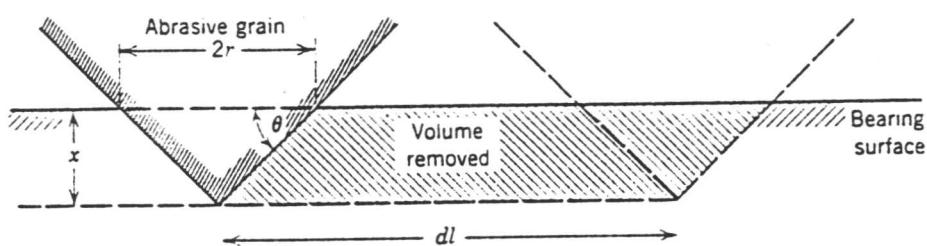
Fig. 3.5: A simplified model representing the material removal due to abrasion.[10]
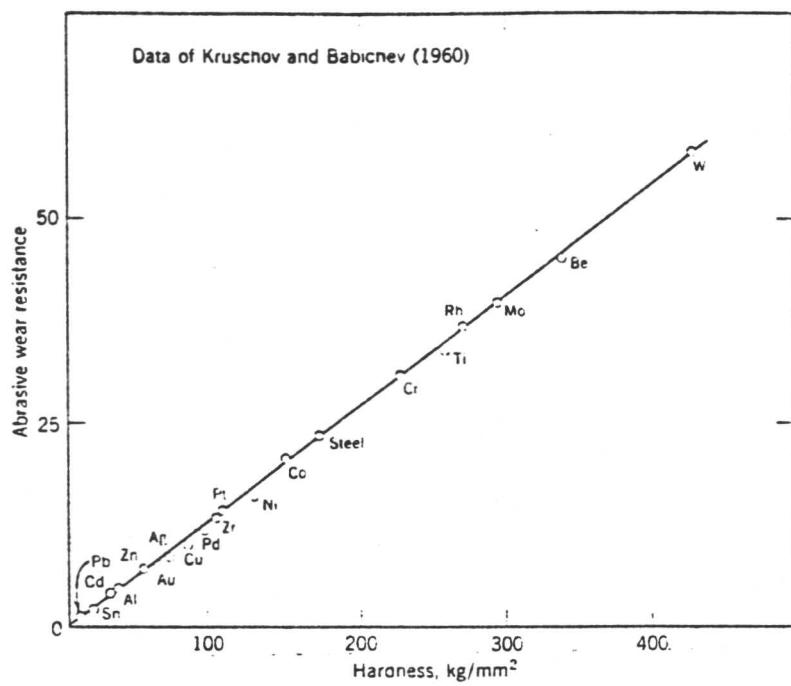
Fig. 3.6: Hardness versus abrasive wear resistance for pure metals in two-body abrasion.[11]
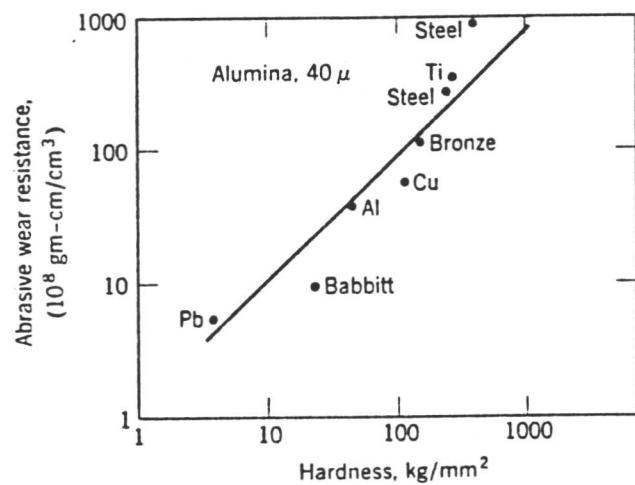
Fig. 3.7: Hardness versus abrasive wear resistance for pure metals in three-body abrasion.[12]

3.6 Effect of Abrasive Properties

1. The Abrasive Hardness

It has been shown that abrasive wear resistance increases as the hardness of the worn material approaches that of the abrasive.[6] This is illustrated in Fig. 3.8 for metallic materials and ceramics. Several suggestions have been made to quantify the critical H_m/H_a (the ratio of the hardness of the material to the hardness of the abrasive) ratio. A general conclusion is that the hardness of a material should be adopted to the abrasive in order to provide the wear occuring in the soft abrasive[2] region.
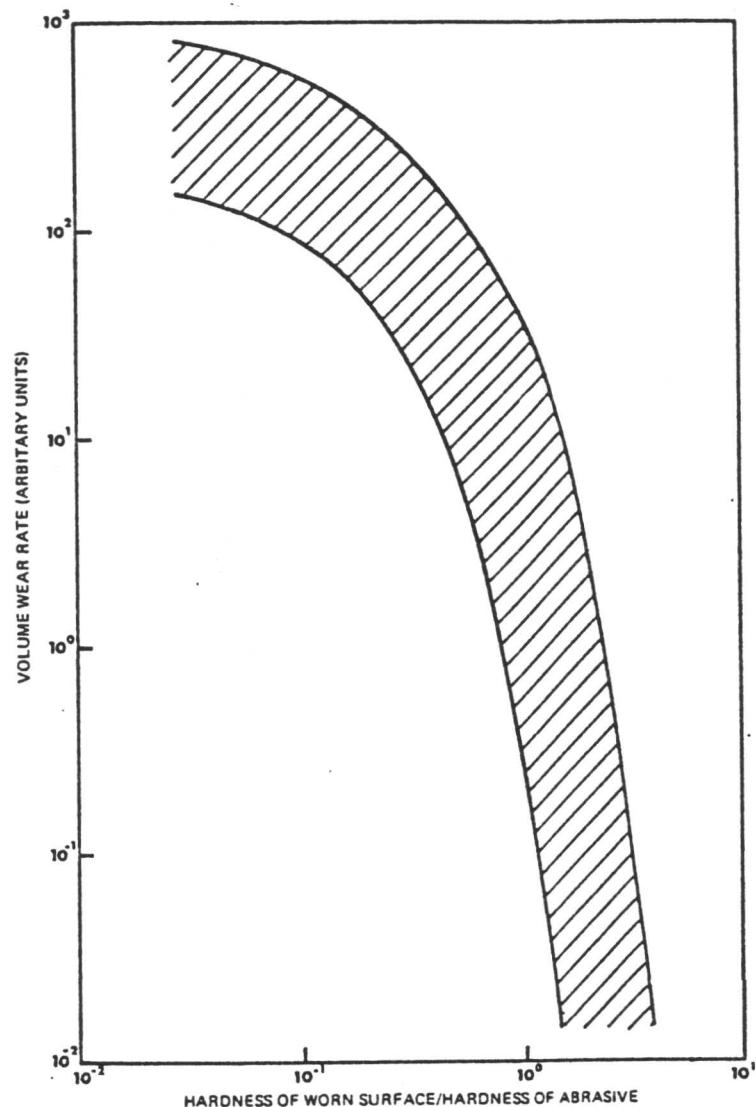
Fig. 3.8: Effect of the H_m/H_a ratio on abrasive wear resistance in metallic materials and ceramics, (worn on 80-100μm bonded abrasives at 1MN/m^2 load).[6]

---

[2]

If the hardness of an abrasive is equal to or less than that of the worn surface, it is called a "soft abrasive".

27

2. The Abrasive Shape

It is now appreciated that sharper (angular) abrasive particles give rise to a higher weight loss when compared with rounded particles. The wear rate with the angular crashed quartz abrasives was found to be between 2 and 5.5 times greater than rounded Ottawa sand due to deteriorating behaviour of angular abrasives.[13] It has recently been reported that the volume loss could be 10 times higher with the angular abrasives in plain carbon and low alloy steels.[14] The cross-sectional area of a groove depends on the particle shape so that the ratio of cross-sectional to projected area of contacts is higher for pyramidal or conical contacts than for spherical contacts. The higher deteriorating effect of angular abrasives is important particularly in carbide containing alloys since preferential abrasion of a matrix phase may lead to unsupported carbides. In addition to that, the sharp edges of the abrasives can cause extensive carbide cracking which is not observed with round abrasives.

3. The Abrasive Size

In a wide range of materials, the wear rate has been shown to increase with the abrasive particle size (Fig. 3.9).[6] The effect is highest for non-metals. The predominant changes in material removal mechanisms are suggested to be responsible for this consequence.[6] A number of possible explanations have been made to clarify the lower wear rate associated with a decrease in the abrasive size. It has been suggested that only a lower fraction of the load is carried with the fine abrasives.[15] The other possibilty is that loose wear debris prevents some abrasives from contacting the material surface. It is quite likely that the worn surface is clogged by wear debris as illustrated in Fig. 3.10. The probabilty for clogging is higher with fine abrasives, and therefore the number of contacts between the abrasives and the worn surface is less than with the coarse abrasives.

4. The Effect of Abrasive Degradation

During abrasion, it is common for the abrasive itself to degrade. This is illustrated in Fig. 3.11 which shows removed-mass as a function of the number of traverses of a steel on 220 grit SiC abrasive paper.[7] The paper rapidly loses efficiency, and after about 1600 traverses it is no longer effective. Experiments dealing with the effect of abrasive degradation on wear resistance showed that the loss of efficiency depends upon the abrasives, and also on the target material.[16] For instance, when Co-based powder metallurgy alloys were tested a second time against SiO_2 abrasives 50 pct. loss in abrasive efficiency was observed. However, the effect of the degradation of the Al_2O_3 abrasives in the same alloys is negligible. On the other hand, the opposite results were observed when 1020 steel was used as a target material.[17]

The experimental results indicate that degradation of the abrasives has a significant influence and this makes it difficult to understand the effect of microstructure on abrasive wear resistance.

28
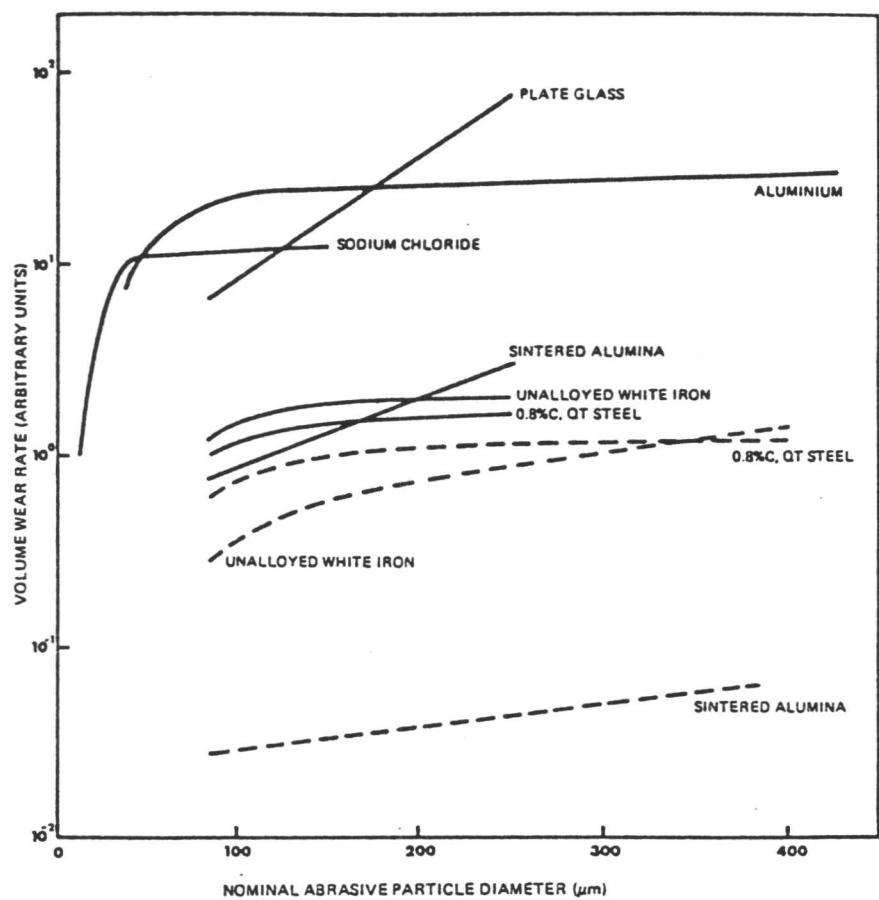
Fig. 3.9: Effect of the abrasive size on abrasive wear resistance; solid lines for SiC abrasives, broken lines for Al_2O_3 abrasives at $1MN/m^2$ load.[6]
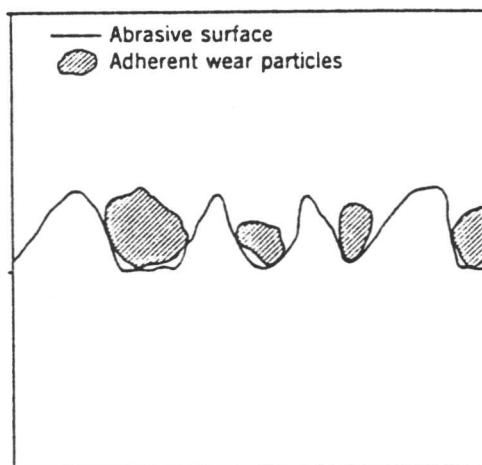
Fig. 3.10: Schematic representation of the worn surface which is clogged by wear debris.

29
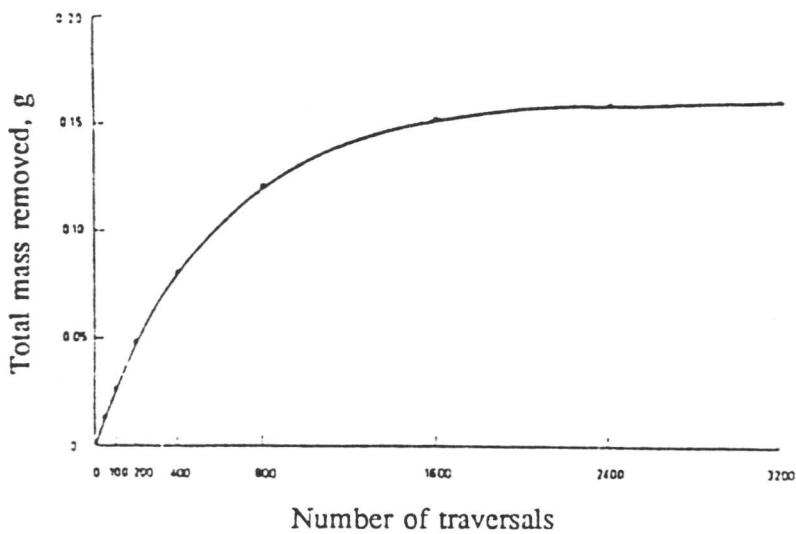
Fig. 3.11: Material removal rate as a function of traverses of a steel on 220 grit SiC abrasive paper.[7]

3.7 Summary

The economic aspects of tribology and the great need for systematic research have been well appreciated. It is necessary, therefore, to understand and improve the knowledge of wear phenomena. Abrasive wear is regarded as being of the greatest industrial significance. The material loss due to abrasion could be minimized if the understanding of the abrasive wear mechanism is achieved.

Material removal mechanisms are generally classified as ploughing, cutting and spalling in the order of increasing brittleness. However, in practical environments it is quite likely that more than one type of wear process occurs simultaneously, and also that each process may involve a number of wear mechanisms.

Applied abrasives have a significant influence in the material removal mechanisms. The attack angle could change the removal mechanism from ploughing to cutting. Abrasive hardness, abrasive shape, and abrasive orientation also have effect on the material loss. These variables could be so effective that they may make understanding of the fundamental aspects of wear rather complex and difficult. Therefore, a great number of parameters have to be taken into account in order to understand the wear phenomenon.

3.8 References

1) H. SUH, and N. SAHA: Fundamentals of Tribology, 1980.
2) Metals Handbook, 9th edn, 1983, ASM, USA.
3) Wear Control Handbook, ASM, New York, 1980.
4) A. P. MERCER: 'The effects of atmospheric humidity and oxygen on the wear of metals by fine abrasives', Ph.D. Thesis, 1985, University of Cambridge.
5) K. H. ZUM GAHR: 'Microstructure and Wear of Metals', Tribology Series. 10, New York, 1987.
6) M. A. MOORE: 'Abrasive Wear', in Proc. Conf. 'Fundamentals of Friction and Wear of Materials', 4-5 October 1980, Pittsburgh Pennsylvania, ASM.
7) T. O. MULHEARN, and L. E. SAMUELS: Wear, 1962, **5**, 478.
8) K. HOKKIRIGAWA, and Z. Z. LI: in Proc. Conf. 'Wear of Materials 1987', New York 1987, Am. Soc. Mech. Eng., 585.
9) N. P. SUH: 'Abrasive Wear', in Proc. Conf. 'Fundamentals of Friction and Wear of Materials', 4-5 October 1980, Pittsburgh Pennsylvania, ASM., 43.
10) E. RABINOWICZ: 'Friction and Wear of Materials', John Wiley and Sons, New York, 1965.
11) M. M. KRUSCHOV: in Proc. Conf. 'Lubrication and Wear', Institution Mech. Eng., London, 1957, 655.
12) E. RABINOWICZ, L. A. DUNN, and P. G. RUSSELL: Wear, 1961, **4**, 345.
13) M. A. MOORE, and F. S. KING: in Proc. Conf. 'Wear of Materials 1979', New York 1979, Am. Soc. Mech. Eng., 275.
14) P. A. SWANSON, and R. W. KLANN: in Proc. Conf. 'Wear of Materials 1981', New York 1981, Am. Soc. Mech. Eng., 379.
15) S. W. DATE, and S. MALKIN: Wear, 1976, **40**, 223.
16) T. H. KOSEL, and N. F. FIORE: J. Materials for Energy Systems, 1981, **3**, 7.

4. THE EFFECT OF PROCESS VARIABLES ON DEPOSIT PROPERTIES

4.1 Introduction

The properties and quality of the weld hardfacing deposits depend on welding techniques and conditions so that it is necessary to understand the effect of welding variables on hardfacing deposit characteristics and properties. Typical variables in the usual welding techniques are arc current, arc voltage, polarity, electrical stickout, travel speed, electrode angle, electrode diameter, and preheat temperature. The effect of these variables on dilution, deposit geometry, penetration, hardness, deposition rate, porosity, and microstructure have been examined by several authors.

In this section the influence of each variable for all combinations of the other variables will be examined.

4.2 Deposit Geometry

The cross-sectional area of the bead reinforcement and of the fused nugget, along with their dilution, width, heat affected zone, and the penetration are shown schematically in Fig. 4.1.
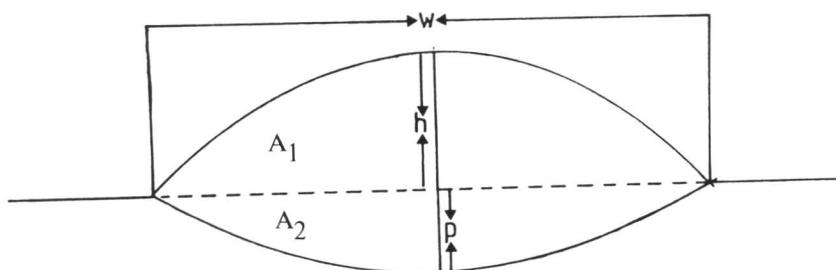
Dilution = $A_2/A_1 + A_2$
w = bead width
h = bead height
p = penetration

Fig. 4.1:   Dimensions of weld bead

Experimental studies have shown that the arc voltage has the greatest effect in determining the height and width of the deposit bead. Rense et al.[1] examined the effect of welding variables on the chemistry, microstructure, and wear behaviour of high Cr and Mo containing white cast irons deposited by arc welding, using a self-shielding flux-cored wire electrode. An increase in the

voltage was found to widen the deposits. They suggested that an increase in potential (at fixed current), leads to a corresponding increase in the arc gap,[1] and spreads the arc on the substrate, resulting in wider beads. Similar results were found by Ellis and Garrett,[2] and Kuznetsov et al.,[4] who found wider deposits with higher voltages, for the flux cored arc welding, and submerged arc surfacing techniques respectively.

It has also been demonstrated that wider beads are obtained when the current is increased, almost irrespective of welding technique.[1-5] However, other variables such as the arc polarity may alter the influence of current levels on the width of the bead, as shown by Ellis and Garrett.[2] They found that increasing the current has a more profound effect on the deposit width with the direct current electrode positive (DCEP) operation than with the direct current electrode negative (DCEN) operation.[2] They suggested that most of the heat is generated at the cathode (in the case of DCEP this is the substrate), and subsequently a wider region of the substrate is melted. This phenomenon was found to be more pronounced at higher voltages and currents. However, most of the heat is generated at the electrode with DCEN, and an increase in the arc current has only a small effect on the deposit width. In fact, they observed a decrease in the deposit width with increasing the arc current at lower arc voltages (deposit width decreased to ≈9mm from ≈11mm when the arc current was increased to 360A from 240A at 24V). Although a decrease in the deposit width was attributed to the distribution of heat in the arc, the reasons are not clear. On the other hand, it has been shown that in the case of DCEN, the deposition rate is increased by an appreciable amount, for example, in the submerged-arc welding surfacing technique.[6] For instance, at 800A the deposition rate is about 9kg/hr, with DCEP, but 13kg/hr with DCEN.[6] Since an increase in the deposition rate is accompanied by a reduction in the deposit height and width, Ellis and Garrett's results could be explained on the basis of the effect of the deposition rate.

Attempts have also been made to verify the effect of the travel speed[2,3,5,7] and preheat[2] on the width of the deposit. Experimental results show that an increase in the travel speed leads to a decrease in the deposit width regardless of the surfacing technique used. However, only relatively little work characterising the effect of preheat on the deposit width has been carried out. Ellis and Garrett[2] suggest that preheating slightly increases the deposit width, probably because more of the heat input then goes into melting.

It is widely believed that the arc current, voltage, and travel speed are the parameters which have a strong influence on the height of the weld bead.[1-5,7] Experimental observations clearly show that the height of the bead is increased with arc current, irrespective of surfacing technique.[2-5,7] This effect is more profound (especially at high current levels), with the DCEN operation in the flux cored arc welding process (FCAW),[2] since most of the heat is then

---

[1]   The arc gap is defined as the distance from the molten tip of the electrode core wire to the surface of the molten weld pool.

[2]   In DCEP, the work is the negative pole, and the electrode is the positive pole of the welding arc. On the other hand, the opposite is the case for DCEN.

33

generated at the electrode leading to an increase in the burn-off rate (the weight, or the length of electrode melted in unit time). Subsequently, when the molten metal falls into the melt pool, spreading is inhibited due to surface tension, resulting in taller deposits.

Although the arc voltage is not found to have a great effect on the height of the bead deposited using electric arc surfacing technique,[3] lower voltages tend to give higher deposits in FCAW technique.[2] However, in submerged arc surfacing technique the bead height increased with the arc voltage.[4] This discrepancy in the experimental results may arise due to the different range of current and voltage levels used in the two studies.

It is now appreciated that travel speed has a significant influence on the bead height. Experimental results have demonstrated a considerable decrease in the deposit height with increasing travel speed.[2,3,5,7]

Since the heat input is directly proportional to the arc voltage and current, some authors have attempted to establish a relationship between the deposit geometry and the heat input. Rense et al.[1] showed that the bead height and area increase with current at constant heat input. In addition, when the level of heat input was high ($\approx$ 5MJ/m), it was found that the area per bead increased more rapidly with current, probably due to the effect of deposition rate, which is a function of both the current and travel speed. In fact, their results showed a linear relationship between the cross-sectional area per bead and the wire speed/travel speed ratio, which is proportional to the deposition rate.[3] They suggested that the bead area is not only a function of the heat input, but also depends upon the deposition rate. However, it should be borne in mind that the linear effect of the heat input on the deposition rate is well established.[8] Therefore, the apparent sensitivity of the bead area to the deposition rate could be explained by this linear relationship. For this reason, it is possible to relate directly the influence of the heat input to the bead area. This conclusion was supported by Clark,[9] who showed that the area of the bead is directly proportional to the heat input, as confirmed by experimental results and theoretical analysis.[9] There is considerable evidence that the burn-off rate (for a given electrode diameter) is proportional to the welding current, and the relationship is given as follows:

$$\pi r^2 L \rho \ / t = KI \qquad \qquad .....(1)$$

where, r is the radius of the electrode core wire, L is the length of the electrode consumed in time t, ρ is the density, K is a proportionality constant[4] and I is the welding current. The heat input is represented by equation 2;

$$H = IV/v \qquad \qquad .....(2)$$

where V is the arc voltage, and v is the travel speed. Combining the equations 1 and 2 gives;

$$H = \pi r^2 \rho \ V/K \quad L/D \qquad \qquad .....(3)$$

---

[3]   The correlation coefficient was found to be 0.98, indicating a perfect relationship between cross-sectional area per bead, and deposition rate.

[4]   The proportionality constant, K, depends upon different parameters, such as specific heat, density, and melting point of the material.

By considering the bead area A, equation 3 yields the following result;

$$H = \rho \ VA/K \qquad .....(4)$$

It is apparent from equation 4 that simple proportionality is present between the heat input and the bead area, as supported by experimental results. An attempt has been made by Clark[9] to correlate the relationship between the heat input and width, and the height of the bead. His regression analysis showed that the width and height of the bead are both proportional to the square root of the heat input. This implies that the bead shape is independent of the heat input over the range of experimental data used (heat input varied from 0.29 KJ/mm, to 3.0 KJ/mm). Alberry and Jones[10] made a similar attempt with the manual metal arc welding technique, and found very good correlation between the heat input and the single bead height, h, (with a correlation coefficient 0.94) and the single bead width, w, (correlation coefficient 0.98) over the range of 1-1.6 KJ/mm heat input. Their regression equations are given as follows;

$$h = 0.0014 \ \eta \ (VI / v) + 1.09 \qquad .....(5)$$
$$w = 0.00825 \ \eta \ (VI / v) + 3.26 \qquad .....(6)$$

where η is the arc efficiency.

Thorpe[11] examined the effect of the welding parameters on deposit characteristics, for the automatic open-arc welding technique using high-Cr austenitic irons. The weld profile (Fig. 4.2.) was expressed empirically as a function of the current-voltage ratio (I/V).
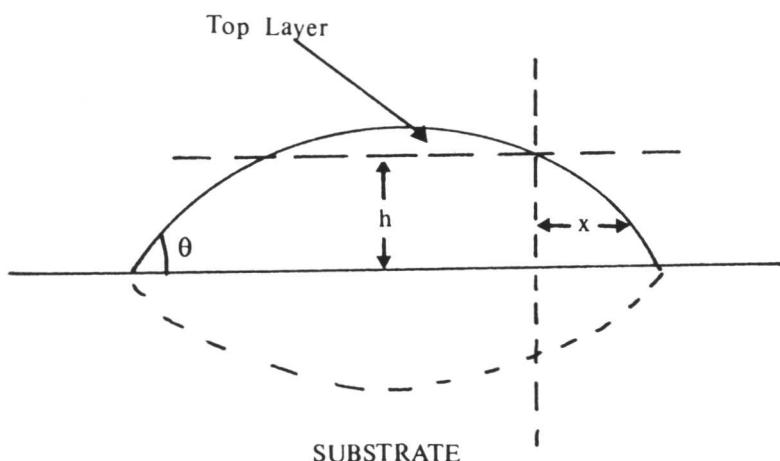

Fig. 4.2:   The profile parameter, x/h, and contact angle, θ.[11]

Rather suprisingly, Thorpe found a good correlation, and also proposed the optimum conditions that provide the desired microstructure for the best abrasive wear resistance. However, although he found that the welding speed strongly influenced the weld profile (with an increase in the

35

welding speed the profile was decreased), this has not been taken into account in determining the optimum conditions.

Although the heat input influences the bead area, it has little effect on the contact angle (see Fig. 4.2). The contact angle determines the tendency of a deposit to spall off under service conditions. If this angle is small, then discontinuous penetration is inevitable, resulting in subsequent spalling.[1,11] It has been reported that the contact angle depends upon the current (an increase in the current led to a decrease in the contact angle[1]). It is suggested that an increase in current (when the heat input is maintained constant) in conjunction with a decrease in voltage causes a decrease in the arc gap, and gives smaller arc spread, resulting in low contact angles.[1] Thorpe[11] suggested that the current-to-voltage ratio, I/V, should be less than 10 AV^{-1}, for satisfactory results. In different work a 60° contact angle was considered as a lower limit for the prevention of spalling,[1] although direct evidence of such an observation is lacking.

There have been numerous attempts to establish the relationship between the welding parameters and the penetration depth. Although it is a matter of argument, the arc voltage, arc current, travel speed, electrode stickout, polarity, and preheat are all found to influence the penetration depth. Experimental results show that an increase in arc voltage and current [2-4,12,13] (i.e., an increase in heat input) lead to higher penetration since more of the substrate reaches the melting temperature.

Any increase in the travel speed causes the heat input to drop and leads to a reduction in the penetration depth, (Eq. 2) as confirmed by experimental results.[2] Therefore, attention has been confined to the parameters which involve the arc current, voltage, and travel speed. Jackson introduced the "welding technique performance factor" $(I^4 / vV^2)^{1/3}$, which was found to be proportional to penetration in the submerged arc, and MMA welding techniques.[14-16] This factor was found to correlate well enough with Clark's experimental results.[9] In addition to this when Clark compared his results with the work of Watanabe and Satoh,[17,18] who showed that the penetration is proportional to $I/\sqrt{v}$ (for a given plate thickness), agreement was fairly good. From these experimental results it is reasonable to assume that the penetration depth is a function of the heat input, because (as seen from Eq. 2), the arc voltage, current, and the travel speed are all involved in determining the heat input. This argument was supported by experimental results which showed that penetration is approximately proportional to the square root of the heat input.[11,14]

The effect of the electrode stickout on the penetration depth was investigated by Baggerud.[19] He found a significant decrease (from 4.8mm, to 2.8mm) in the penetration depth when the electrode stickout increased (from 10mm to 40mm), probably through its effect on the welding current (which decreased to 255A from 365A). The importance of the correct electrode stickout was emphasized by Nugent,[20] who suggested that shorter extension gives less resistance heating in an electrode, and leads to a deeper penetration. On the other hand, enlargement of wire extension causes a subsequent increase of melting of the electrode by 15-100% (depending upon

36

the welding current), leading to a lower penetration and an increase in the life-time of hardfacing alloys.[21]

Although the contrary is claimed,[22] it is generally accepted that the negative arc polarity decreases the penetration depth,[2,6] probably through its influence on the deposition rate, which is increased with negative polarity, leading to a decrease in the heat input.

As one would expect, penetration increases with preheat temperature as confirmed by experimental results.[2,9]

So far, attention has been confined to the influence of welding parameters on the deposit geometry. However, optimum conditions have to be examined by considering the effect of these parameters on different deposit characteristics. Therefore the following sections are aimed at this problem.

4.3 Dilution

The composition of a weld is influenced by the mixing of the base material with the deposit and this effect is called dilution. The dilution is generally measured by the percentage of base material, or previously deposited weld material in the weld bead.

Many attempts have been made to establish the relationship between welding parameters and dilution, since abrasive wear resistance is influenced strongly by the dilution. The implications of different dilution levels in dealing with the abrasive wear resistance will be discussed in detail later on. In this section the influence of the welding parameters on dilution, particularly for arc welding techniques will be discussed.

Experimental results indicate that arc voltage, arc current, travel speed and polarity have a significant influence on the dilution, whereas electrode stickout, electrode diameter and preheat are found to have relatively little effect. Although there is considerable evidence concerning the influence of the arc current, discrepancies between the experimental results have been so great in many instances as to make a general conclusion impossible. One would think that higher currents would give rise to more dilution, because the heat input then increases causing deeper penetration, which in turn should mean a higher level of dilution. Direct evidence of such an effect has been observed by a large number of investigators,[3,5,7,13,19,23,24] and supported by others.[25,26] However, Ellis and Garrett[2] showed that the role of the arc current depends upon the arc polarity (whether DCEP or DCEN). They found that an increase in the arc current significantly decreases the dilution with DCEN operation (when the arc current increased to ≈ 360 A, from ≈ 240 A, dilution decreased to 29%, from ≈ 40%). One of the important features of the DCEN operation is its significant influence on the deposition rate. There is considerable evidence that the negative polarity increases the deposition rate of the electrode by a large amount,[2,6,25,27] which in turn means that more material is deposited, giving a less dilution.[2] In contrast to the DCEN operation, only a slight increase was found in the dilution when raising the arc current in the DCEP operation with FCAW technique.[2] This is consistent with the fact that for the DCEN operation, most of the heat is generated at the substrate. Therefore, a wider area is melted than with the

DCEP operation, leading to a higher dilution. However, Thorpe[11] has found no systematic relationship between the arc current and the dilution (at each of the three deposited layers) with either DCEN or DCEP operations, using austenitic Fe-Cr-C alloys. It should be noted that he used the DCEP operation in the first layer in order to obtain good penetration and the DCEN technique was used in the second and third layers to minimize remelting of the previous deposits. This complexity in his experiments make results difficult to interpret. The recent results of Rense et al.,[1] and Noble[28] are in conflict with these observations. They both found a decrease in the dilution with increasing the arc current in arc welding techniques. Rense et al.[1] examined the effect of arc-welding variables on the deposit characteristics, using a self-shielding flux cored wire electrode, in high Cr iron base hardfacing alloys (Fe-22.1Cr-2.9C-3.0Mo-0.3Si-0.3Mn). They found a linear decrease in the dilution with increasing the arc current (in the range of ≈ 200- ≈ 400A), at three different heat inputs (1, 2, 5 MJ/m). Although their statistical analysis showed a good correlation (correlation coefficient 0.86), they suggested that the heat input dependence of the data is not random. Similarly, dilution was found to decrease with increasing the current in the work of Noble,[28] who examined the effect of welding variables in the flux-cored arc welding technique, with iron base hardfacing alloys. He varied the current between 250-450 A, while other parameters were kept constant (voltage at 24V, with 20mm electrode stickout, and at 1.8 mm/s travel speed). Although he used the DCEP operation, the increase in the arc current led to a decrease in dilution. He suggested that at high current a large weld pool develops, which lessens the influence of the arc, resulting in a low penetration and less dilution. It is most probable that discrepancies between the different experimental results occur due to the influence of other parameters (e.g. electrode stickout, travel speed, preheat) on the dilution.

Dilution is found to increase with the arc voltage, as confirmed by a great number of authors.[2,3,11,26,28,29]5 This is expected since a higher arc voltage is associated with an increase in the burn-off rate, and in the heat input. It should be pointed out that Ellis and Garrett[2] incorrectly interpreted the data concerning the effect of the voltage on dilution. They wrote: "An increased arc voltage tends to decrease penetration and (hence dilution)" (their references 20, 22, 25). In contrast, Kuznetsov et al.[4] clearly showed an increase in the penetration depth with increasing arc voltage in the submerged arc surfacing technique (their reference 25). In the work of Yuzvenko and Kirilyuk[30] (their reference 22) there was no direct study about the relationship between the arc voltage and dilution. As a third reference they refer to Farmer's work[31] (their reference 20). In this it is reported that if an excessively long arc is applied (which in turn means an increase in the arc voltage), and molten metal is overexposed to the air, Cr and C can be lost giving a less alloyed microstructure (similar to a highly diluted alloy). Apparently this study does not indicate the effect of the arc voltage on the dilution level, because the molten weld pool is deliberatly overexposed to the air causing less Cr and C concentration in the deposit.

---

5   It should be noted that the work of Thorpe[11] showed an increase in dilution up to 28V, and then it was found to remain almost constant.

Travel speed is determined by the relative velocity between the electrode, and the workpiece.[29] Increasing the travel speed leads to a decrease in the heat input (see Eq. 3), penetration, and dilution.[26] However, experimental studies using the flux cored arc welding technique show that an increase in the travel speed gives rise to higher dilutions.[2,23] This discrepancy is not obvious, and indicates that further work is necessary.

Electrode stickout (or extension) is the distance between the electrode nozzle contact tip, and the end of the electrode.[29] Electrical resistance of the electrode increases with this distance, resulting in a decrease of the welding current. Therefore, longer stickout gives smaller penetration, and a lower dilution. In contrast, short stickout results in a greater penetration (and dilution) than long stickout. It is now appreciated that too long an extension is associated with a lower arc voltage. Therefore this leads to a poor weld-bead shape, and a shallow penetration.[29] For these reasons, it is necessary to establish a quantitative relationship between the electrode extension and dilution. However, many of the results are based on the qualitative comparisons. For example, Baggerud[19] found a significant decrease of the penetration (from 4.8mm to 2.8mm) with increasing the electrode stickout, from 10mm to 40mm. Similarly, Thorpe[11] found a systematic increase of the volume fraction of the primary carbides with the electrode stickout (when the electrode stickout increased to 80mm from 35mm, volume fraction of the primary carbides increased to ≈ 18% from ≈12%), indicating that a lower dilution is achieved with a longer stickout. He proposed that the decrease in arc voltage with longer stickout is a major effect for less dilution. Noble[28] observed the same phenomenon in the flux cored arc welding technique with high Cr austenitic iron deposits. He found a slight increase in the primary Cr carbide volume fraction with electrode stickout, indicating a lower dilution. Although the influence of the electrode stickout is well established, various stickout lengths are reported for better results (e.g. less dilution, higher wear resistance). This conflict could be explained by the influence of the stickout on the dilution. For instance, Noble[28] found a decrease in dilution with increasing stickout. However, his experiments showed better wear resistance with a higher dilution. Apparently, his choice for the best stickout length would be the one, which gives a relatively low dilution. On the other hand, in many cases a lower dilution led to higher wear resistance. In these cases, obviously different stickouts would be suggested. This discussion suggests that in order to chose the optimum conditions the effect of microstructure on the deposit properties (e.g. oxidation, corrosion, and wear resistance) should be discussed.

The influence of the wire feed rate (for a given electrode diameter), is well established through its effect on the arc current. The results show that increasing the wire feed rate leads to higher current levels, resulting in more dilution.[29,32,33]

Also the electrode diameter has an influence on the dilution. If two wires with different electrode diameters are operated at the same amperage, the smaller will give a greater dilution, and a higher deposition rate than the larger, because of its higher current density (amperages per unit of cross-sectional area).[33] Therefore, the choice of the size of electrode wire depends upon

unit of cross-sectional area).[33] Therefore, the choice of the size of electrode wire depends upon the required properties such as the deposition rate and bead profile.

Preheating is generally preferred in the high carbon equivalent steels, (C content exceeds about 0.30%) in order to eliminate crack formation in the heat-affected-zone (HAZ). It also decreases the cooling rate, and promotes transformation of austenite to soft pearlite instead of hard martensite.[5] Dilution was found to increase with preheating temperature,[2,5,9] due to the fact that preheated substrate increases the amount of base metal melted at the same heat input. As one would expect, the greater the amperages with preheating gave rise to a much higher dilution.[5]

4.4 Deposition Efficiency and Deposition Rate

Deposition efficiency is the ratio of weight of metal deposited to the weight of electrode consumed.[33] It depends on the welding processes and welding parameters such as the arc current, voltage, polarity, and electrode stickout. The influence of these parameters was examined by Ellis and Garrett,[2] for flux cored arc deposition of hardfacing alloys. They showed that the deposition efficiency significantly increases with the arc current, probably due to an increase in metal transfer across the arc. Conversely, increasing the arc voltage led to a substantial drop in the deposit efficiency. They suggested that at higher arc voltages the amount of spatter increases, resulting in a lower deposition efficiency. Also, increasing the electrode stickout gave rise to a slight drop in the deposition efficiency (when they increased the stickout to 36mm from 24mm, deposition efficiency reduced to ≈ 69% from ≈ 72%). Although this effect is not significant, it is well known that an excessive stickout leads to spatter, and irregular action in the flux cored arc welding process.[29]

The weight of material deposited per unit of time is known as a deposition rate.[33] During surfacing by a variety of arc welding processes the arc current, voltage, polarity, travel speed, preheat, electrode diameter, electrode composition, and electrode stickout are all found to have a great effect on the deposition rate. The influence of the arc current on the deposition rate is well established, through its increasing effect on the burn-off rate at higher amperages.[29] Furthermore, there is considerable evidence that an increase in the deposition rate is associated with higher arc currents, irrespective of welding techniques.[2,6,7,23,29,33] At the same welding currents, the deposition rate was found to increase when the DCEN operation is used in the flux cored[2] and submerged arc welding[6] techniques. This is because, most of the heat is concentrated at the electrode with the DCEN operation resulting in a higher melting rate, and higher deposition rate. In FCAW technique the influence of the arc voltage was studied by Ellis and Garrett,[2] who found a decrease in the deposition rate with increasing the arc voltage. They suggested that this decrease is associated with increasing the dilution and reducing the deposition efficiency at higher voltages.

When the travel speed is decreased, the amount of filler metal deposited per unit length increases,[26,29] giving a higher deposition rate as confirmed by experimental results.[2]

40

It is of interest here, to examine the influence of electrode size, and electrode stickout on the deposition rate. For a given amperage, if two electrodes have the same mode of metal transfer, the electrode with a small diameter will have a higher current density and a higher deposition rate than a larger diameter electrode.[29,33]6 This conclusion was supported by experimental results as well.[29]

The influence of the electrode diameter can be explained through its effect on the electrode. Increasing electrode extension leads to a greater amount of heating, higher melting, and higher deposition rate.[33]

In addition to the parameters discussed above, surfacing with two electrodes,[33] and alloyed wires[23] (for a given electrode stickout) are reported to have an increasing effect on the deposition rate.

4.5 Microstructure

It is appreciated that the microstructure of iron-based hardfacing alloys has a significant influence on the oxidation, corrosion, and abrasive wear resistance. Therefore, it is vital to establish the effect of the welding parameters on the microstructure for achieving the best performance of hardfacing alloys during service. The variation of the microstructure in these alloys depends primarily on the Cr/C ratio. The liquidus surface and the phase relationships between the liquid phase and the primary solid phases have been investigated in the Fe rich region, C<6wt% Cr<40wt%, of the Fe-Cr-C system.[34,37] Thorpe and Chicco[34] studied a large number of alloys in order to establish the Fe-Cr-C liquidus surface and solidification sequences. They have shown that different solidification sequences are observed by the variations in total composition. In regard to iron-based hardfacing alloys, two different solidification sequences are most commonly observed. High Cr and high C containing alloys give a typical solidification sequence in which $(Fe,Cr)_7C_3$ carbide is the first phase to solidify in the absence of any stronger carbide forming elements such as Nb and Ti. As the temperature decreases, a eutectic reaction occurs with the liquid phase transforming to austenite and more M_7C_3 carbides. After this stage, solid-state phase transformations may occur depending upon the chemical composition and cooling conditions. In the second category (generally low Cr and low C containing alloys), austenitic dendrites are the first crystals to separate from the melt. As the temperature decreases, either M_7C_3 or M_3C eutectic carbides may form together with more austenite, depending upon the actual alloy composition. Although the liquidus surface and equilibrium solidification sequences in Fe-Cr-C system are well established, it is quite difficult to predict the final microstructure that results from arc welding. These alloys are deposited in several layers in order to prevent dilution, and to provide a buffer effect which accommodates differences in thermal expansion between the substrate and the top layer. Martensite formation has been observed in the

---

6 It should be noted that a larger diameter electrode can carry more current and therefore allow a higher deposition rate.

highly diluted areas at and near the weld metal/base metal junction.[38,39] The formation of martensite can cause an expansion in volume, leading to a significant compressive stress[40] and catastrophic failures.[38] A typical example of martensite formation is illustrated in Fig. 4.3.

Fig. 4.3: Optical micrograph of the first layer in the Fe-23.11Cr-3.75C-9.38Nb-0.42Mn-1.29Si (wt%), containing a high amount of martensite.[41]

The magnitude of the martensite formation depends upon welding technique and welding parameters, as well as thermal and mechanical properties of the substrate and deposit materials. Factors such as thermal conductivity, thermal expansion coefficient, hardness, and yield strength of the base metal and the deposit material are known to influence the formation of martensite.[40] A substrate with a higher thermal conductivity and heat capacity increases the probability of the martensite formation at the interfaces (substrate/deposit interface).[40] Similarly a base metal with a low yield strength may contribute to stress relaxation, reducing the chance of the stress-induced martensite formation. Although the deposition of further layers reduces the stresses in the surface of the deposit, thermal expansion coefficients of these layers should be between the base metal and top layer. Otherwise, intermediate layers cannot maintain their cushion effect.

In Fe-based hardfacing alloys there is a strong influence of the welding variables such as, the arc current, voltage, polarity, electrode stickout on the microstructure of multilayer deposits.

Among these variables, the arc current and voltage were reported to have the most significant influence. For instance, increasing the arc voltage changes the microstructure of Fe-Cr-C hardfacing deposits by influencing dilution.[9] It was found that for almost all the welding conditions used, the[7] first layer revealed hypoeutectic microstructure containing cellular dendrites in a matrix of austenite and M_7C_3. The second layer was found to be strongly dependent upon the arc voltage and current, through the effect of these variables on the dilution. At the highest voltage and lowest current levels (34V, 250A), the second layer was found to be fully eutectic having a cellular growth of the fibrous of $\gamma + M_7C_3$ phase. However, at a lower voltage and higher current conditions, hypereutectic microstructure (containing primary needle type M_7C_3 carbides in a matrix of eutectic mixture of austenite, and more M_7C_3) was found. Thorpe observed some undisolved Cr-rich particles at the top layer. Similar particles were observed by Powell[42] with the MMA welding process. He found that M_7C_3 carbides grew (in a spine like manner) from these particles, causing a nonuniform carbide distribution. Also, giving a slightly hypoeutectic, or even eutectic alloy, rather than hypereutectic, due to reduced total Cr content in the deposit. It was suggested that the increase in the amount of undissolved Cr rich particles was accompanied by an inhomogenous weld pool occuring as a result of lower inputs and faster welding speeds.[42] The effect of the arc current and the heat input on microstructure was investigated by Rense et al.,[1] in Fe-Cr-C type hardfacing alloys with an arc-welding process. They observed that the heat input caused a coarsening of the primary austenite dendrites. However, the volume fraction of the eutectic microconstituent (austenite/M_7C_3 interdendritic network) was found to be strongly dependent upon the current, rather than the heat input. At higher currents (lower dilution) microstructure was observed to contain large M_7C_3 primary carbides, but hypoeutectic microstructure was found at lower currents (higher dilution). These results are consistent with the work of Noble,[28] who examined the effect of the arc current and voltage on the microstructure of high Cr austenitic iron base deposits with the FCAW technique. He observed hypereutectic microstructure with higher currents, through both layers. In contrast, an increase in the voltage gave rise to a less volume fraction of the primary M_7C_3 carbides, implying a higher dilution.

The effect of the electrode stickout was studied by Noble,[28] and Thorpe.[11] They both found that volume fraction of the primary M_7C_3 carbides increased with the electrode stickout length. This is because, lower stickout decreases the arc voltage and dilution, as discussed previously.

The results show that the microstructure of iron-based hardfacing alloys could be controlled by welding parameters. The significance of these results is obvious since an understanding of the influence of welding parameters on the microstructure is of great importance for material selection in hardfacing applications.

---

[7]   In this work four voltage levels (25, 28, 31, 34V), and four current levels (250, 280, 310 and 350A) were chosen.[9]

43

4.6 Conclusions

Hardfacing materials may be deposited by a wide range of welding processes, and their properties depend strongly on the welding procedure and conditions used. For example, the arc voltage and current have a significant influence in determining the deposit geometry. Although an increase in these variables leads to the formation of wider and taller deposits, other parameters such as the arc polarity, the travel speed, and the preheat are also found to affect weld bead geometry. The heat input, which is a function of the arc current, voltage and the travel speed is found to increase the weld bead area.

An understanding of the effect of the variables which influence the penetration depth is particularly important for hardfacing alloys since the level of dilution is determined by the degree of penetration. Ideally, dilution should be kept to a minimum in order to optimize the properties of the cladded material. Results have shown that the penetration increases with the arc voltage and current, and decreases with the travel speed. Even though the effects of the electrode stickout and the arc polarity have been reported, more work is needed to establish a relationship between these variables and the penetration depth.

The hardfacing material is mixed with the molten base metal during welding leading to a certain degree of dilution. An increase in the arc current, and the voltage gave rise to a high level of dilution, as expected. However, the arc polarity was found to play a significant role. For instance, the dilution was found to decrease with increasing the arc current when the direct current electrode negative technique was applied. This is because the deposition rate of the electrode is increased leading to a high deposition rate and therefore less dilution. A quantitative assessment of the influence of arc polarity would also be very useful so that the deposit geometry and the level of dilution can be simultaneously controlled.

The microstructure of hardfacing alloys is primarily influenced by the dilution since the mixing of the original material with the base metal changes the composition, and consequently the properties. As an example, the wear resistance in high chromium containing iron-based harfacing alloys was found to decrease with increasing dilution. So, for a given electrode, the welding parameters should be chosen to provide the best possible microstructure for any given application.

4.7 References

1) C. E. C. RENSE, G. R. EDWARDS, and H. R. FROST: J. Materials for Energy Systems, 1983, **5**, 149.
2) T. ELLIS, and G. G. GARRETT: Surface Engineering, 1986, **2**, 55.
3) A. I. KOMAROV, V. D. KHODAKOV, and A. S. ZUBCHENKO: Welding Production, 1981, **28**, 33.
4) L. D. KUZNETSOV, M. R. NIKOLAENKO, and N. A. GRINBERG: Automat. Weld., 1980, **33**, 47.
5) H. ZENTNER: Welding and Metal Fabrication, 1976, **44**, 208.
6) A. M. HORSFIELD: Welding and Metal Fabrication, 1977, **45**, 507.
7) S. FORSBERG, and U. EKSTROM: Welding Review, November, 1982.
8) C. S. DIMBYLOW, and K. M. CHIPPERFIELD: Welding and Metal Fabrication, 1983, **51**, 229.
9) J. N. CLARK: Mat. Sci. and Techn., 1985, **1**, 1069.
10) P. J. ALBERRY, and W. K. C. JONES: 'A computer model for the prediction of heat affected zone microstructures in multi-pass weldments', 1979, Central Electricity Generating Board Report, R/M/R282.
11) W. R. THORPE: Metals Forum, 1980, **3**, 62.
12) K. THORN: Met. Constr., 1982, **14**, 128.
13) G. G. CHERNYSHEV, I. S. MARKUSHEVICH, and M. R. NIKOLAENKO: Svar. Proizvod, 1984, **9**, 19.
14) C. E. JACKSON: Weld. J., 1960, **39**, 129.
15) C. E. JACKSON: Weld. J., 1960, **39**, 177.
16) C. E. JACKSON: Weld. J., 1960, **39**, 225.
17) M. WATANABE, and K. SATOH: Weld. J., 1955, **24**, 512.
18) M. WATANABE, and K. SATOH: Weld. J., 1956, **25**, 18.
19) A. BAGGERUD: Met. Const. and British Weld. J., 1969, **1**, 18.
20) B. T. NUGENT: Met. Const., 1982.
21) J. JARACZ: Przegl. Spawalnictwa, 1984, **36**, 10.
22) A. VAN-BEMST, R. A. DAEMEN, and D. H. YOUNG: Met. Cons. and British Weld. J., 1969, **1**, 109.
23) F. GURDET: Welding and Metal Fabrication, 1983, **51**, 505.
24) D. L. KHANNA, M. I. KHAN, and P. C. GUPTA: Tool and Alloy Steels, 1980, **14**, 333.
25) W. WAHL: Surfacing J., 1980, **11**, 2.
26) P. SYMONS: Surfacing J., 1983, **14**, 45.
27) J. STROMBERG: Welding and Metal Fabrication, 1982, 212.
28) D. N. NOBLE: 'The effect of flux-cored arc welding conditions on microstructure and abrasive wear resistance of two iron-based hardfacing alloys', Welding Inst. Res. Report 7856.02/86/479.3, November 1986.
29) Metals Handbook, 9th edn, 1983, ASM, USA.
30) Yu. A. YUZVENKO, and G. A. KIRILYUK: Automat. Weld., 1974, **27**, 55.
31) H. N. FARMER: Met. Eng. Q., 1975, **15**.
32) M. IRMLER, and V. STENKE: in Proc. Conf. 'Welding and Cutting 84', Frankfurt, 1984.
33) Welding Handbook, W. H. KEARNS, ed., 7th edn., **2**, American Welding Society, 1978.
34) W. R. THORPE, and B. CHICCO: Metall. Trans. A, 1985, **16A**, 1541.
35) N. R. GRIFFING, W. D. FORGENG, and G. W. HEALY: Trans. TMS-AIME, 1962, **224**, 148.
36) D. M. KUNDRAT, M. CHOCHOL, and J. F. ELLIOTT: Metall. Trans. B, 1984, **15B**, 663.
37) J. D. B. DeMELLO, M. DURAND-CHARRE, and HAMAR-THIBAULT: Metall. Trans. A, 1983, **14A**, 1793.
38) C. P. COOKSON: Surfacing J., 1985, **16**, 125.
39) C. P. COOKSON: Surfacing J., 1985, **16**, 44.
40) Z. BABIAK: Surfacing J., 1985, **16**, 114.
41) S. ATAMERT: CPGS Thesis, University of Cambridge, 1985.
42) G. L. POWELL: Australian Welding Research, 1979, **6**, 16.

Nomenclature

The following nomenclature is used throughout this Chapter.

t	time (s)
λ	thermal conductivity (J s^{-1} m^{-1} K^{-1})
a	thermal diffusivity (m^2 s^{-1})
ρc	specific heat per unit volume (J m^{-3} K^{-1})
q	arc power (J s^{-1})
υ	arc velocity (m s^{-1})
r_b	radius of heat source (m)
z	depth below plate surface (m)
y	distance from the centre of the heat source (m)
T	temperature (K)
T_p	peak temperature in thermal cycle (K)
T_o	preheat temperature (K)
T_m	melting temperature (K)
t_o	time constant (r_b^2 / 4a)
z_o	length constant, given by Equation 4
e	base of natural logarithms (2.718)
w	weld bead width (m)
h	weld bead height (m)
p	penetration depth (m)
d	electrode diameter (m)
A_1	area of bead reinforcement (m^2)
A_2	total melted area (m^2)

46

5. THE PREDICTION OF WELD BEAD DIMENSIONS AND DEGREE OF DILUTION IN ARC WELDING DEPOSITS

5.1 Introduction

It has been demonstrated in Chapter 4 that a wide range of weld bead morphologies and microstructures can be generated in hardfacing deposits by altering the welding variables. The welding conditions, and in particular the rate of cooling the deposited material, have an important influence on microstructure altering the volume fraction of microconstituents, and their chemical compositions. These changes will affect the abrasive wear resistance of the deposit. It is therefore desirable to quantify their effect on weld deposit chemistry, and microstructure in order to obtain optimum wear resistance. An attempt is made in this chapter to predict the weld bead dimensions and the dilution as a function of welding parameters (heat input, travel speed, etc.). The heat flow equations originally derived by Rosenthal for a moving point source,[1] and later modified for a circular disc source,[2] have been used. Rosenthal derived heat flow equations corresponding to thick, fairly thick, and thin plates for a point source moving with constant velocity, v, along the x-axis of a fixed rectangular coordinate (x, y, z) system, as a function of time t (Fig. 5.1).

For thick plates

$$T - T_0 = \frac{q}{2\pi\lambda R} \exp\left\{-\frac{v}{2a}(\xi + R)\right\}$$

.....(1)

for thin plates

$$T - T_0 = \frac{q}{4\pi\lambda\rho c v r'} \exp\left\{-\frac{v}{2a}(\xi + r')\right\}$$

.....(2)

where T_0 is the preheat temperature, λ is the thermal conductivity, q is the arc power, ρc is the specific heat per unit volume, $r^2 = \xi^2 + y^2 + z^2$, $r'^2 = \xi^2 + y^2$, a is the thermal diffusivity, and $\xi = (x - vt)$.

47
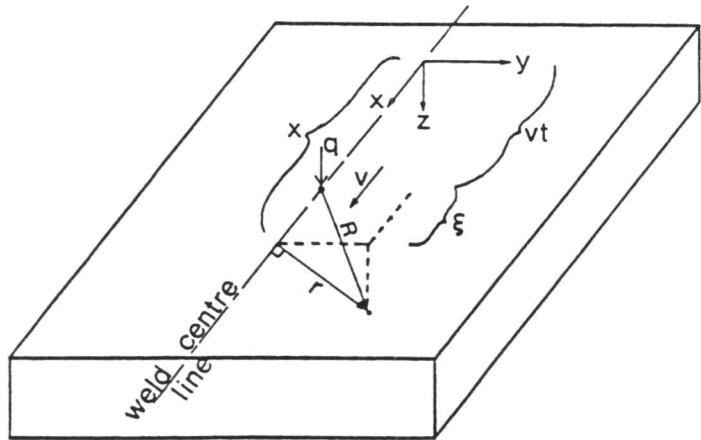
Fig. 5.1: Welding geometry and coordinate systems used for the analysis of Rosenthal equations.[2]

5.2 Modified Rosenthal Equations for a Disc Source

The Rosenthal equations assume that heat is delivered from a point heat source. This means that satisfactory results may not be achieved when large electrodes are used. This shortcoming was overcome when the point source was replaced by a circular disc source of radius r_b.[3] For thick plates it was shown that the temperature cycle $T(y,z,t)$ at a point (y,z) below the surface is well-approximated by the following equations

$$T = T_o + \frac{q/v}{2\pi\lambda[t(t+t_o)]^{1/2}} \times \exp\left[-\frac{1}{4a}\left(\frac{(z+z_o)^2}{t} + \frac{y^2}{(t+t_o)}\right)\right] \quad .....(3)$$

where

$$z_o{}^2 = \left[\frac{r_b}{e}\left(\frac{\pi a r_b}{v}\right)^{1/2}\right] \quad .....(4)$$

$$t_o = \frac{r_b{}^2}{4a} \quad .....(5)$$

The parameter t_o represents the time required for heat to diffuse over the radius of heat source, r_b. The length, z_o, is a distance over which heat can diffuse during the interaction time r_b/v.

48

Note that for thick plates when $r_b = 0$, Equation 3 reduces to the original Rosenthal equation.

5.2.1 The Temperature-Time Profile

The temperature-time profile for a given point in the weld pool was calculated using Equation 3. Typical curves are given in Figs. 5.2a-d corresponding to the points in the weld bead (Fig. 5.2e). The data used for the calculations are given in Table 5.1.
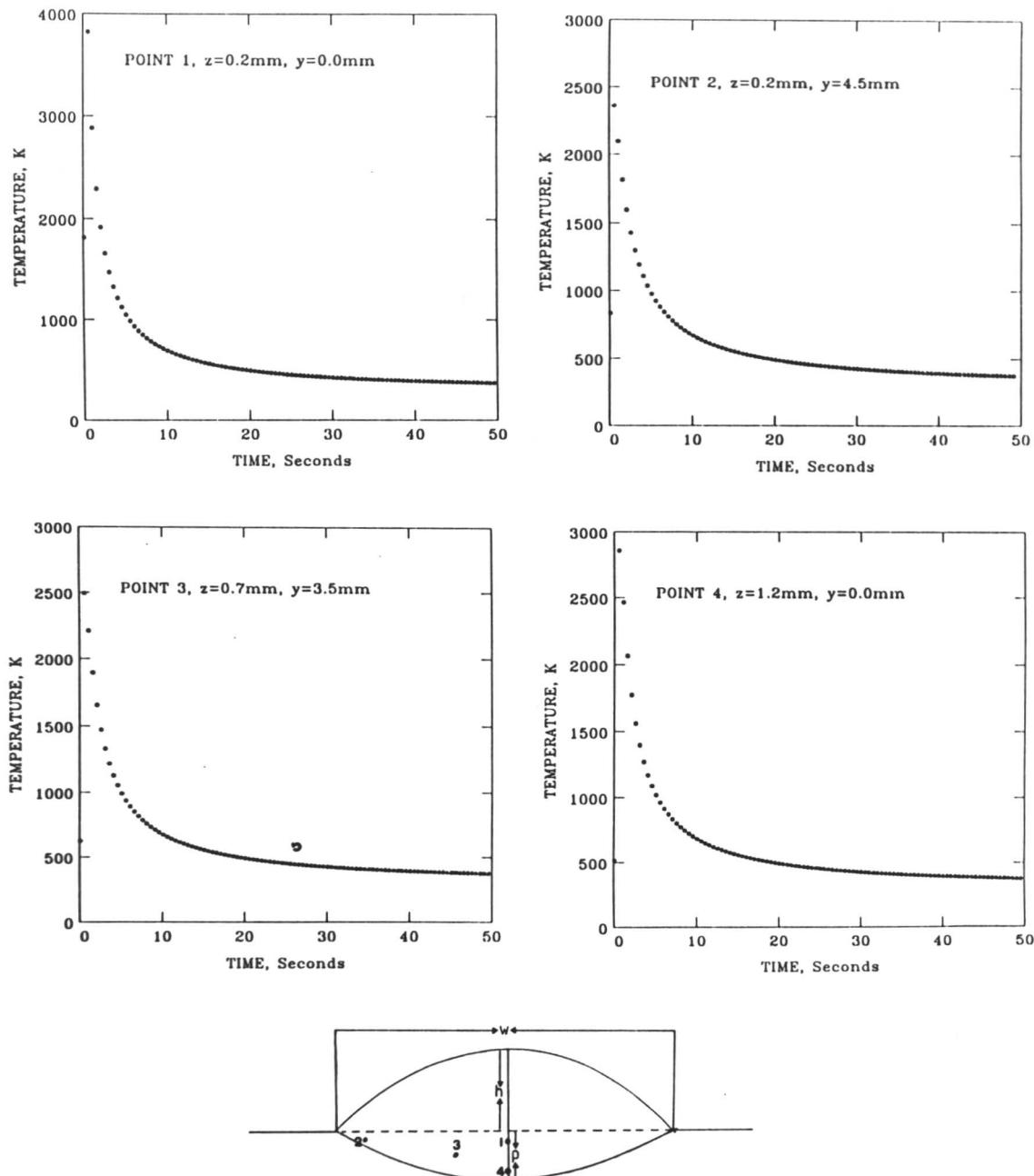

Fig. 5.2: a) Temperature-time profiles; b) corresponding points in the weld bead. The welding conditions are: $q = 1500J/s$, $\upsilon = 4mm/s$, $r_b = 4mm$, and $T_0 = 293K$.

49

Table 5.1: Data used in the calculations for carbon steel base plate.

Property	Symbols	Units	Value
Thermal conductivity	λ	J/msK	41
Thermal diffusivity	a	m^2/s	9.1×10^{-6}
Volume thermal capacity	ρc	J/mK	4.5×10^{-6}
Melting Point	T_m	K	1810

5.2.2 Calculation of the Peak Temperature Achieved During Deposition

The peak temperature, T_p, reached in the thermal cycle for a given point, is calculated by differentiating Equation 3 with respect to time, to give the following parabolic function

$$2at_p(2t_p + t_0)(t_p + t_0) = t_p^2 y^2 + (z + z_0)^2(t_p + t_0)^2$$

$$.....(6)$$

The time (which is the real root of the parabolic function) corresponding to the peak temperature (t_p), calculated when $\partial T / \partial t = 0$. The variations of the peak temperature with distance z is given in Fig. 5.3.
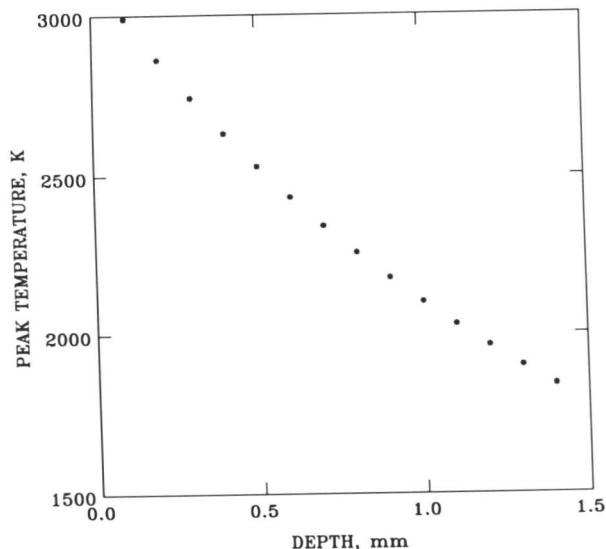

Fig. 5.3: The variations of the peak temperature as a function of z along the weld centre-line. The welding conditions are: q = 1500J/s, υ= 4mm/s, r_b = 4mm, and T_0 = 293K.

50

5.3 Calculations for Weld Bead Dimensions

1. Area of Bead Reinforcement

As discussed in Chapter 4, the area of bead reinforcement is directly proportional to the heat input. This relationship was explained theoretically and the relationship between the heat input and the area of bead reinforcement was represented in Chapter 4 (Eq. 4). In the arc welding processes the area of bead reinforcement can be calculated by considering the total melted deposit as follows;

$$A_1 = (\pi \, d^2 \, /4) \times \text{recovery} \times (\text{feed speed} / \text{welding speed}) \quad \ldots\ldots(7)$$

where d is the electrode diameter. The recovery is defined as the ratio of the weight of deposited metal to the net weight of filler metal consumed. The accuracy of this equation was tested with the experimental data of Clark on MMA deposits (for 5mm electrodes),[3] and by Alberry et al.[4] for TIG deposits. The regression analysis were carried out, and observed values against those calculated are represented in Figs. 5.4a,b. It is clear that the area of bead reinforcement could be satisfactorily calculated through the Equation 7.
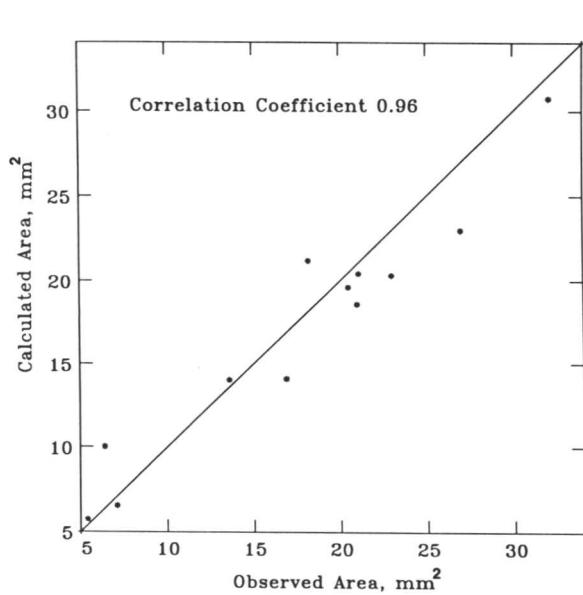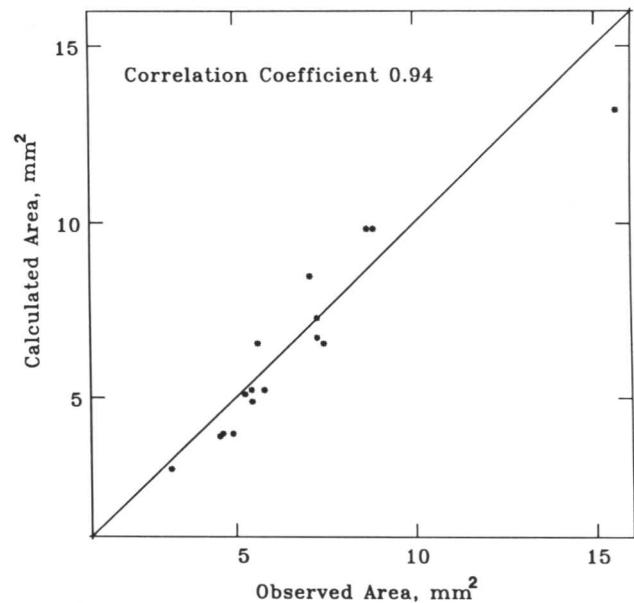
a   b

Fig. 5.4: Calculated bead area versus observed bead area a) data after Clark for the MMA deposits; b) data after Alberry et al. for the TIG deposits. During calculations the radius of the disc source, r_b is assumed to be equal to the electrode diameter for the MMA (5mm), and to the wire diameter for the TIG (1.2mm), process.